

2-14-2014

determining the function of hotdog-fold thioesterases

Yajun Wu

Follow this and additional works at: https://digitalrepository.unm.edu/chem_etds

Recommended Citation

Wu, Yajun. "determining the function of hotdog-fold thioesterases." (2014). https://digitalrepository.unm.edu/chem_etds/49

This Thesis is brought to you for free and open access by the Electronic Theses and Dissertations at UNM Digital Repository. It has been accepted for inclusion in Chemistry ETDs by an authorized administrator of UNM Digital Repository. For more information, please contact disc@unm.edu.

YAJUN WU

Candidate

Department of Chemistry and Chemical Biology

Department

This thesis is approved, and it is acceptable in quality and form for publication:

Approved by the Thesis Committee:

Debra Dunaway-Mariano, Chairperson

Patrick S. Mariano

Charles E. Melançon

**DETERMINING THE FUNCTION OF HOTDOG-FOLD
THIOESTERASES**

BY

YAJUN WU

B.S., Life Science, Wuhan University, China, 2011

THESIS

Submitted in Partial Fulfillment of the

Requirements for the Degree of

Master of Science

Chemistry

The University of New Mexico

Albuquerque, New Mexico

July, 2013

ACKNOWLEDGMENTS

I am very thankful to my wonderful advisor Dr. Debra Dunaway-Mariano for her advice, guidance, and support throughout my graduate studies. I am in awe of her ability to always be available both professionally as a mentor and as a friend. I would also like to thank my committee members, Dr. Patrick S. Mariano, and Dr. Charles Melançon for their valuable feedback regarding my work and their support during my time as a graduate student.

I am also thankful to all of the past and present members of DDM Lab for their friendship, support, discussions, and feedback that everyone has provided throughout my time at the lab. I am particularly indebted to John A. Latham for his guidance and help with techniques and troubleshooting. This work would not have been possible without their constant support and feedback.

I would also like to thank the faculty in the Chemistry and Biological Chemistry Department for being fantastic educators and inspiring me to effectively communicate my work to others.

Additionally, I would also like to thank the administrators in the department for helping me go through this process, reminding me at every step when something is due.

Finally, this work would not have been possible without the complete support of my loving husband, Yao Wan, who has always been by my side. I am also thankful to my family as well as all of the friends that I have been lucky enough to encounter. It is with their love, support, and encouragement that this thesis is in existence.

DETERMINING THE FUNCTION OF HOTDOG-FOLD THIOESTERASES

BY

YAJUN WU

B.S., Life Science, Wuhan University, China, 2011

M.S., Chemistry, University of New Mexico, 2013

ABSTRACT

The enzymes that hydrolyze thioesters to the free acids and free thiols are called thioesterases. Based on the different folding strategy, most thioesterases are classified into two superfamilies: the hotdog-fold enzyme superfamily or alpha/beta-fold hydrolase enzyme superfamily. Hotdog-fold thioesterases share high degree similarity in structure which resembles a “hotdog”.

YigI is one of the last two uncharacterized hotdog-fold thioesterases from *E.coli*. To study the function of YigI, substrate specificity profile was determined by thioesterase activity assay. YigI possesses a preference for long chain acyl-CoA over shorter chain acyl-CoA. The highest activity was found in catalysis of myristoyl-CoA. By alignment with the closest homolog, the uncharacterized tetrameric type AB thioesterase from *Shewanella oneidensis*, the important catalytic residues of YigI were predicted as following: Asp69, Gln56 and His60. Enzyme activity decreased after the site-direct mutagenesis of those residues.

Cytoplasmic acetyl-coenzyme A hydrolase (CACH), also known as acyl-CoA thioesterase12 (Acot12), plays important cellular roles in mammalian fatty acid metabolism through the hydrolysis of acyl-CoA thioesters. Unlike YigI, besides two hotdog domains, CACH contains a steroidogenic acute regulatory (START) domain. The START domain is known as a lipid transporter. Thus, the function and regulation of CACH is of special interest. Chapter three of this thesis focuses on the function of the tandem hotdog-fold domains of CACH. The double hotdog-fold unit of CACH was expressed in *E. coli* and purified. Surprisingly, it was shown to display highest activity towards isobutyryl-CoA rather than acetyl-CoA.

TABLE OF CONTENTS

LIST OF FIGURES.....	viii
LIST OF TABLES.....	xiii
LIST OF ABBREVIATIONS.....	xiv
CHAPTER ONE.....	1
AN INTRODUCTION TO THE HOTDOG-FOLD THIOESTERASE ENZYME SUPERFAMILY.....	1
1.1 Biological function of thioesterases.....	1
1.2 Hotdog-fold thioesterases superfamily.....	3
1.3 Catalytic mechanisms of the hotdog-fold thioesterase	4
1.4 Hotdog-fold thioesterase functions in the model bacterial system <i>E. coli</i>	5
1.5 Hotdog-fold thioesterase functions in humans.....	6
1.6 References	10
CHAPTER TWO.....	13
CHARACTERIZATION OF THE HOTDOG FOLD THIOESTERASE YIGI FROM <i>E.</i> <i>COLI</i>	13
2.1 Introduction	13
2.2 Methods and Materials.....	14
2.2.1 Materials.....	14
2.2.2 Preparation of wild-type <i>E. coli. yigI</i>	15
2.2.3 Determination of the steady state kinetic constants	15
2.2.4 Site-directed mutagenesis	16
2.3 Results and discussion.....	17
2.3.1 Recombinant yigI purification and verification.....	17
2.3.2 YigI substrate specificity profile determination	19
2.3.3 Site-directed mutagenesis	28
2.3.4 Discussion.....	30
2.4 References.....	31
CHAPTER THREE.....	32
DETERMINE THE FUNCTION OF HOTDOG-FOLD THIOESTERASES “CYTOPLASMIC ACETYL-COENZYME A HYDROLASE” (CACH) FROM HUMAN.....	32

3.1 Introduction	32
3.2 Materials and Methods.....	33
3.2.1 Materials	33
3.2.2 Expression and purification of CACH.....	34
3.2.3 Steady-state kinetic analysis of CACH.....	35
3.2.4 Protein-Lipid Overlay Assay	35
3.2.5 Co-immunoprecipitation of recombinant StarD15 and CACH.....	36
3.3 Results and discussion.....	37
3.3.1 CACH purification and verification.....	37
3.3.2 CACH substrate screen for determination of biochemical function.....	38
3.3.3 Interaction with lipids	40
3.3.4 Site-directed mutagenesis	44
3.3.5 Discussion.....	48
3.4 References.....	50

LIST OF FIGURES

Figure 1.1	Secondary structure diagram of the ‘canonical’ α/β hydrolase fold ¹ . White cylinders and gray arrows indicate α helices and β strands respectively. Black dots represent the location of the conserved catalytic residues.....1
Figure 1.2	The active sites for the 4-hydroxybenzoyl-CoA thioesterase from <i>Pseudomonas sp</i> strain CBS3 (AA type) (left) and the 4-hydroxybenzoyl-CoA thioesterase from <i>Arthrobacter sp</i> strain AU (AB type) (right). Asterisks represent residues that belong to the second subunit of the dimer ⁵3
Figure 1.3	The general base catalysis (top) and nucleophilic catalysis (bottom) in the hotdog-fold thioesterase catalysis.....4
Figure 1.4	Domain organization of human type I and type II acyl-CoA thioesterases (ACOTs). Closest homologues (THEM4 and THEM5) are included for comparison ⁹6
Figure 1.5	Domain organizations of human Type II acyl-CoA thioesterases (ACOTs). Closest homologues (THEM4 and THEM5) are included for comparison. HD is short for hotdog domain; START is short for steroidogenic acute regulatory protein (StAR)-related lipid transfer (START) domain; THEM is short for thioesterase superfamily member ¹⁰8

Figure 2.1	Evolutionary tree of YigI. Conversed neighbor genes were shown.....	14
Figure 2.2	Molecular weight determined by SDS-page. 1, centrifuge cell precipitant after French press; 2, cell lysis before centrifuge (whole cell) 3, centrifuge cell supernatant after French press; 4, 5, 6, are different fractions from the Ni column chromatography.....	17
Figure 2.3	Molecular weight determined by Mass Spectrometer.....	18
Figure 2.4	(top) FPLC size exclusion chromatography elution profile, (bottom left) SDS-PAGE of fractions 6, 7, 8 and 9, and (bottom right) calibration plot using protein molecular weight standards.....	19
Figure 2.5	The molecular structure of selected acyl/aryl-coenzyme compounds for the YigI substrate screening.....	20
Figure 2.6	Lineweaver Burk plots measured for YigI-catalyzed hydrolysis of (A) hexanoyl-CoA, (B) octanoyl-CoA, (C) decanoyl-CoA, (D) lauroyl-CoA (E) myristoyl-CoA and (F) palmitoyl-CoA. See Materials and Methods for details.....	21
Figure 2.7	YigI homolog from <i>Shewanella oneidensis</i> (PDB accession code 3E8P). The yellow and cyan colored subunits form one dimer and the green and magenta colored subunits for the other dimer. The two dimers are arranged back-to-back (sheet-to-sheet) to form the tetramer.....	23

Figure 2.8 A. *S. oneidensis* (PDB accession code 3E8P) YigI homolog (type AB).
 B. YdiI (type AB) (PDB accession code 1VI8), C. Ybdb (type AB) (PDB accession code 1VH9), D. PaaI (type AB) (PDB accession code 2FS2), E. YbaW (Type AA) (PDB accession code 1NJK), F. YbgC (type AA) (PDB accession code 1S5U), G. Haemophilus influenza YciA homolog (type AB)(PDB accession code 1YLI), H. Double hotdog TesB (TEII) N-terminal catalytic domain (type AB) (PDB accession code 1YLI)24

Figure 2.9 Surface representations of the *S. oneidensis* (PDB accession code 3E8P) YigI homolog tetramer. Coloring is the same as that used in Figure 2.8. The catalytic Asp is colored white, the channel on the right (yellow) is the pantethiene binding site and the channel to the left (red, green and blue) is the site where the aliphatic tail is expected to bind.....25

Figure 2.10 The residues that line the walls of the aliphatic tail binding pocket in the modeled *E. coli* YigI (left panel) and in the structure of the *S. oneidensis* (PDB accession code 3E8P) YigI homolog (right panel). Carbon atoms are colored black, oxygen red and nitrogen blue. The catalytic Asp is colored magenta. The carbon atoms of the three residues that form the bridge over the pocket are colored cyan.....26

Figure 2.11	The catalytic site of the <i>S. oneidensis</i> (PDB accession code 3E8P) YigI homolog. The Asp68, Thr100, Tyr107, Asn55, Gly60 and His59 residues are shown in stick and the carbon atoms are colored cyan, oxygen atoms red and nitrogen atoms blue.....27
Figure 2.12	SDS-PAGE gel analyses of the YigI mutants containing fractions (A) D69Q, (B) Q56A, (C) H60A, (D) D69E pictured in the gel stained with Coomassie blue dye. See Materials and Methods for details.....28
Figure 3.1	Domain organizations (up) and crystal structure (down) of Acot121.....32
Figure 3.2	SDS-PAGE gel analysis of the CACH containing fractions pictured in the gel stained with Coomassie blue dye.....37
Figure 3.3	Molecular weight determined by Mass Spectrometer.....37
Figure 3.4	The molecular structure of selected acyl/aryl-coenzyme compounds for the CACH substrate screening.....38
Figure 3.5	Lineweaver Burk plots measured for CACH-catalyzed hydrolysis of (A) butyryl-CoA, (B) isobutyryl-CoA, (C) hexanoyl-CoA, (D) octanoyl-CoA. See Materials and Methods for details.....39

Figure 3.6	Protein–lipid overlay assays in which PIP Strips or Membrane Lipid Strips were separately treated with 2 $\mu\text{g}/\text{mL}$ ACOT12, 1 $\mu\text{g}/\text{mL}$ StarD15 domain or 1 $\mu\text{g}/\text{mL}$ CACH domain (purified as described above), in PBS-T and then imaged. The lipid positions are identified in the key. (Acot12 and StarD15, Latham, unpublished data).....41
Figure 3.7	Polyphosphoinositide metabolisms.....41
Figure 3.8	Protein–lipid overlay assays in which PIP Arrays or Sphingo Arrays (Echelon Bioscience Inc.) were separately treated with 2 $\mu\text{g}/\mu\text{L}$ ACOT12 or 1 $\mu\text{g}/\text{mL}$ StarD15 (purified as described above), in PBS-T and then imaged. The lipid positions are identified in the key. (Latham, unpublished data).....42
Figure 3.9	Western blots of the protein fraction eluted from CACH antibody-functionalized agarose beads incubated with 150 μg of CACH and 100 μg of StarD15. Lane 1 was treated with anti-CACH and lane 2 was treated with anti-StarD15. Lane 3 is the protein from the control in which CACH was omitted and treated with anti-StarD15. (middle+/+, Latham, unpublished data).....43
Figure 3.10	SDS-PAGE gel analyses of the CACH mutants containing fractions (A) D31A, (B) E205A pictured in the gel stained with Coomassie blue dye. See Materials and Methods for details.....45

Figure 3.11	Cysteine residues nearby active site. Yellow color represents atom S which shows cysteine residues location.....	47
Figure 3.12	kinetics background study of wild-type CACH was measured using the DTNB spectrophotometric assay at pH 7.5 and 25 °C.....	48

LIST OF TABLES

Table 2.1	Steady-state kinetic constants measured for YigI-catalyzed hydrolysis of various acyl-CoA substrates monitored by DTNB coupled reaction in 50 mM HEPES at pH 7.5 and 25 °C. N/A is “no detectable activity” ($k_{cat} < 1 \times 10^{-4} \text{ s}^{-1}$).....22
Table 2.2	Steady state kinetics study of YigI mutants-catalyzed hydrolysis of myristoyl-CoA substrate monitored by DTNB coupled reaction in 50mM HEPES at pH 7.5 and 25 °C.....29
Table 3.1	Steady-state kinetic constants for CACH catalyzed hydrolysis of acyl-CoA was measured using the DTNB spectrophotometric assay at pH 7.5 and 25 °C. N/D is not determined constant.....40
Table 3.2	Steady state kinetics study of CACH single mutants-catalyzed hydrolysis of isobutyryl-CoA substrate monitored by DTNB coupled reaction in 50mM HEPES at pH 7.5 and 25 °C.....46

LIST OF ABBREVIATIONS

Acots	Acyl-CoA thioesterases
ACP	acyl carrier protein
Ala or A	alanine
Asp or D	aspartic acid
ATCC	American Type Culture Collection
ATP	adenosine 5'-triphosphate
BSA	Bovine Serum Albumin
CACH	cytoplasmic acetyl-coenzyme A hydrolase
4-CBA	4-chlorobenzoic acid
CoA/CoASH	coenzyme A
Cys or C	cysteine
DNA	deoxyribonucleic acid
DI H ₂ O	Distilled and deionized water
DTNB	5', 5'-dithio-bis-(2-nitrobenzoic acid)
E	enzyme
<i>E.coli</i>	<i>Escherichia coli</i>
EXPASY	expert protein analysis system
FPLC	fast protein liquid chromatography
FabA	β -hydroxydecanoyl thiolester dehydratase
Gln or Q	glutamine
Glu or E	glutamate
h	hour

4-HBA	4-hydroxybenzoyl-CoA
4-HBT	4-Hydroxybenzoyl-CoA thioesterases
HD	hotdog domain
HEPES	4-(2-Hydroxyethyl)-1-piperazineethanesulfonic acid
His or H	histidine
IP	immunoprecipitation
IPTG	isopropylthio- β -galactoside
K	rate constant
K _{cat}	enzyme turnover rate
kDa	kilo-Dalton
K _m	Michaelis-Menten constant
L	liter
LB	Luria-Bertani
M	molar
min	minute
mM	millimolar
mL	milliliter
MS	mass spectrum
MW	Molecular Weight
NCBI	National Center for Biotechnology Information
OD	optical density
PA	phosphatidic acids
PaaI	Phenylacetyl-CoA thioesterase
PAGE	polyacrylamide gel electrophoresis

PBS	Phosphate Buffered Saline
PBST	PBS solution with Tween 20
PCR	polymerase chain reaction
PDB	protein data bank
pfu	plaque forming units
PtdIns or PIP	Phosphatidylinositol
SDS	sodium dodecyl sulfate
S	substrate
SEC	size exclusion chromatography
sec or s	second
Ser or S	serine
SM	sphingomyelin
START	steroidogenic acute regulatory protein
THEM	thioesterase superfamily member
Tyr or Y	tyrosine
μL	microliter
μM	micromolar
UV	Ultraviolet
WT	wild type
V_{max}	maximum velocity
yigI	thioesterase from <i>E.coli</i>

CHAPTER ONE

AN INTRODUCTION TO THE HOTDOG-FOLD THIOESTERASE ENZYME SUPERFAMILY

1.1 Biological function of thioesterases.

Thioesters are produced by esterification between a carboxylic acid and thiol and they are important for energy production in cells. Thioesterases (EC 3.1.2.2) are enzymes that hydrolyze thioesters to the free acids and free thiols. The hydrolysis reaction produces free thiols, and free carboxylic acids that vary in size, shape and polarity. Thiols can be coenzyme A, glutathione, the cysteine residue of proteins, or the pantetheine unit of the holo-acyl carrier protein (ACP).

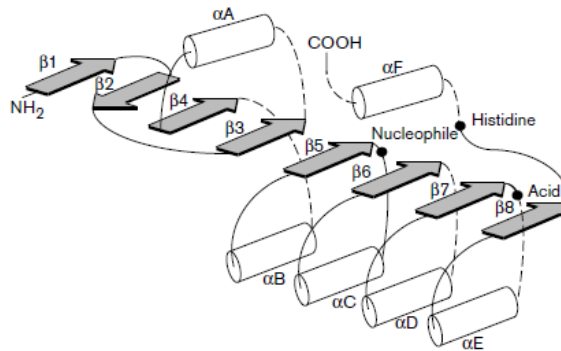


Figure 1.1 Secondary structure diagram of the ‘canonical’ α/β hydrolase fold¹. White cylinders and gray arrows indicate α helices and β strands respectively. Black dots represent the location of the conserved catalytic residues.

Most thioesterases belong to the hotdog-fold enzyme superfamily or alpha/beta-fold hydrolase enzyme superfamily¹. Both superfamilies express thioesterases activity in most cellular compartments such as endoplasmic reticulum, cytosol, mitochondria, and peroxisomes. By maintaining appropriate levels of acyl-CoA, CoA and free fatty acids, they play important roles in lipid metabolism and energy genesis².

The 'canonical' α/β hydrolase fold (Figure 1.1) has been described as an eight parallel β sheet surrounded by α helices on both sides. The catalytic sites are always highly conserved. The conserved active site Ser residue, located after strand $\beta 5$, functions as a nucleophile during catalysis. For general base catalysis, a carboxylate residue located after strand $\beta 7$ is used. It in turn forms a hydrogen bond the conserved histidine residue located after the last β strand. Numerous alpha/beta-fold thioesterases have been studied both structurally and biochemically. There are many X-ray structures of alpha/beta-fold thioesterases deposited in the Protein Data Bank.

1.2 Hotdog-fold thioesterases superfamily

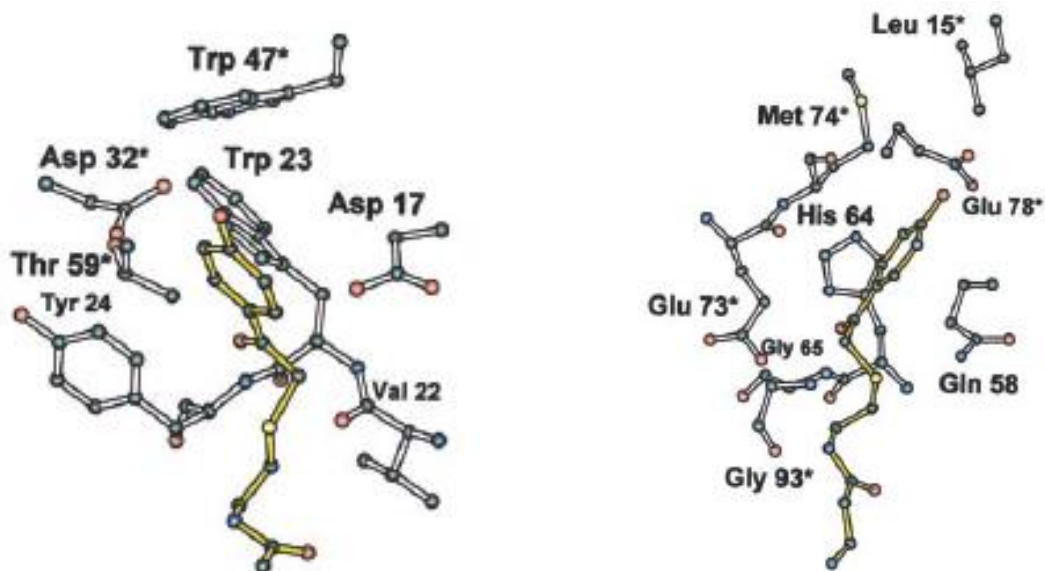


Figure 1.2 The active sites for the 4-hydroxybenzoyl-CoA thioesterase from *Pseudomonas* sp strain CBS3 (AA type) (left) and the 4-hydroxybenzoyl-CoA thioesterase from *Arthrobacter* sp strain AU (AB type) (right). Asterisks represent residues that belong to the second subunit of the dimer⁵.

The hotdog-fold was first discovered by studying the crystal structure of β -hydroxydecanoyl thiolester dehydratase (FabA) in *E. coli*³. The name of “hotdog-fold” comes from the structure resembling a hotdog. The long central helix is the “sausage” and 5 or 6 highly curved antiparallel β -sheets forms the “bun” that encases the helix. A dimer is the minimal biological units as the active site requires residues from both subunits.⁴

To catalyze the hydrolysis of thioester, the carboxylate residue is required to serve as base or nucleophile while the backbone amide NH of a residue positioned at the N-

terminus of the α -helix polarizes the thioester C=O via hydrogen bond formation. Based on different location of the catalytic carboxylate residue and amide residue, thioesterases are categorized into two catalytic motifs: type AA and type AB. For type AA, the catalytic carboxylate residue (Asp17) and α -helix residue (Trp23) are on the same subunit of the dimer. However, for the type AB, the catalytic carboxylate residue (Glu73) and α -helix residue (His64) are on the different subunits of the dimer.⁵

1.3 Catalytic mechanisms of the hotdog-fold thioesterase

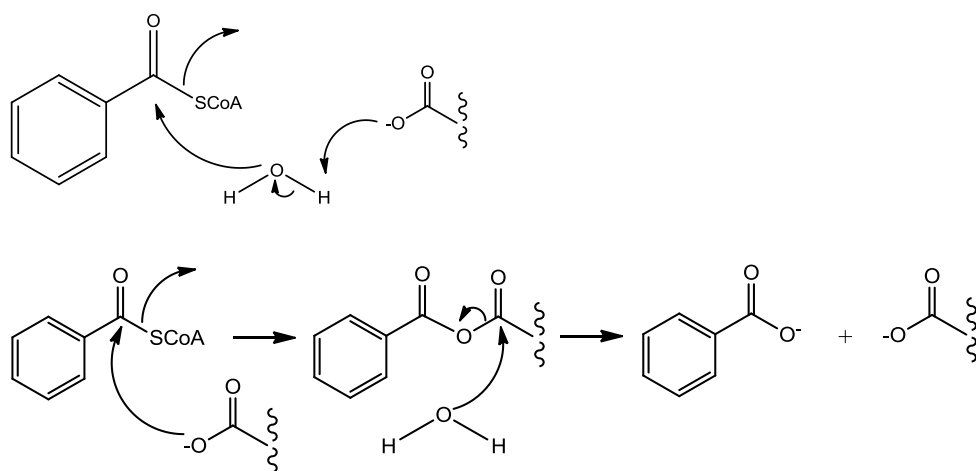


Figure 1.3 The general base catalysis (top) and nucleophilic catalysis (bottom) in the hotdog-fold thioesterase catalysis

The thioesterases belong to different subfamilies of hotdog fold proteins as they differ in their substrate specificities. However, the catalytic strategy is similar (Figure 1.3).

For general base catalytic mechanism, the carboxylate residue activates the water nucleophile for attack at the substrate thioester group. For nucleophilic catalysis, the

carboxylate residue attacks the thioester carboxyl group to form a mixed anhydride intermediate, which in turn hydrolyzed by attack of a solvent water molecule.

1.4 Hotdog-fold thioesterase functions in the model bacterial system *E. coli*

Due to varied substrate specificities, hotdog-fold thioesterases belong to different subfamilies. Some of these subfamilies are well studied while some are not.

4-Hydroxybenzoyl-CoA thioesterase (4HBT) functions in pathway which converts the environmental pollutant 4-chlorobenzoate to the metabolite 4-hydroxybenzoate⁴. It has been characterized both biochemically and structurally. Based on different modes of quaternary association, CoA binding sites and catalytic architecture, 4HBT can be divided into two classes: 4HBT-I and 4HBT-II. In the case of 4HBT-I, AA type tetramers are formed, while 4HBT-II enzymes form AB type tetramers⁵.

The YbgC-like thioesterase exhibits activity on short chain acyl-CoA in the gamma-proteobacterium *Haemophilus influenza*⁶. As YbgC-like thioesterases belong to the tol-pal cluster, a well conserved operon across gram-negative bacteria, it plays an important role in maintenance of cell envelope integrity⁷.

PaaI thioesterases function in the phenylacetic acid catabolic pathway. PaaI thioesterases purified from *Thermus thermophilus* and *E. coli* have been characterized both structurally and biochemically. Similar to the 4HBT-II subfamily, PaaI thioesterases form AB type tetramers⁸. YbdB and ydiI are also type AB tetramers. YbdB functions as a housekeeping enzyme for the enterobactin biosynthetic pathway, by hydrolyzing mischarged EntB and EntF. YdiI on the other hand serves in the menaquinone pathway by hydrolyzing the

pathway intermediate 2,4-dihydroxynaphthoyl-CoA. The *tesB* is active in the hydrolysis of fatty acyl-CoA and fatty acyl-holoACP substrates. YbaW functions in the fatty acid β -oxidation pathway by functioning as a housekeeper through the liberation of CoA from dead-end degradation products (e.g., 3, 5-tetradecadienoyl-CoA). My first project was the characterization of *yigI*, the one remaining *E. coli* hotdog fold thioesterase with unassigned function.

1.5 Hotdog-fold thioesterase functions in humans

Acyl-CoA thioesterases (Acots) play important cellular roles in mammalian fatty acid metabolism through the hydrolysis of fatty acyl-CoA thioesters to release free fatty acid and coenzyme A⁹.

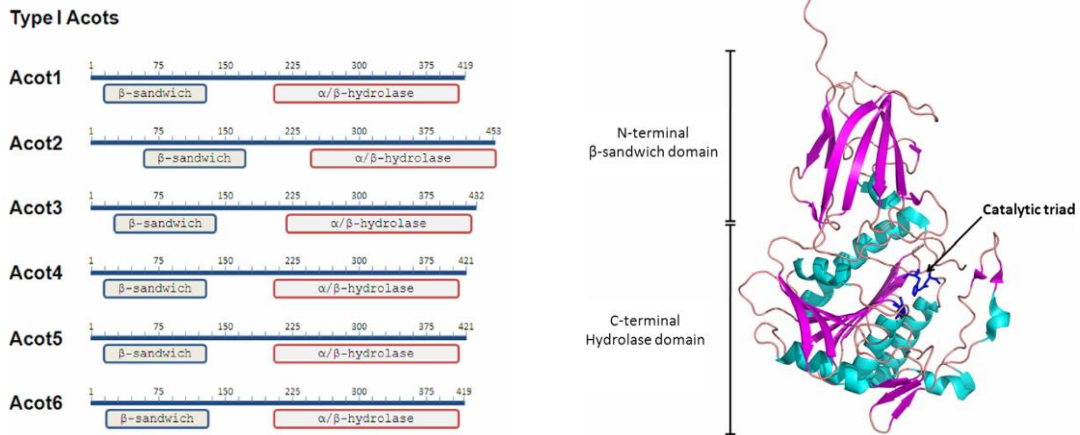


Figure 1.4 Domain organization of human type I and type II acyl-CoA thioesterases (ACOTs). Closest homologues (THEM4 and THEM5) are included for comparison⁹

The activity of Acot was first discovered in the 1950s. As the rapid development of techniques in the following years, several different families of Acots were characterized. Based on the different folds, Acots are divided into two families: Type I thioesterases and Type II thioesterases¹⁰.

Type I thioesterases (Acots 1-6), share sequence and fold with the α/β -hydrolase superfamily (Figure 1.4). Acot1, a cytosolic enzyme, catalyzes the hydrolysis of long chain saturated fatty acyl-CoA¹¹. Acot2, a mitochondrial enzyme, shares several functional characteristics, because the sequence identity between Acot1 and Acot2 is 93%. Thus, Acot2 also favors long chain acyl-CoA¹². As a peroxisomal enzyme, Acot3 possesses the highest activity against palmitoyl-CoA. Another peroxisomal enzyme, Acot4 has a very broad range of substrate specificity. It acts from short chain to long chain acyl-CoA, from saturated to unsaturated acyl-CoA. However, the highest activity shows on catalysis of succinyl-CoA¹³. Acot5, exhibiting highest activity for decanoyl-CoA, has not been reported found in humans. Acot6 is also a reported peroxisomal enzyme. The best substrates published for Acot6 are phytanoyl-CoA and pristanoyl-CoA¹⁴. As shown in Figure 1.4, Type I thioesterases present high level similarity in structure. The members of Type I thioesterases all contain an N-terminal β -sandwich domain which is predicted to be important for regulating the catalysis efficiency. C-terminal of Type I thioesterases is a α/β hydrolase domain. All of the catalytic residues are located within the C-terminal α/β hydrolase domain.

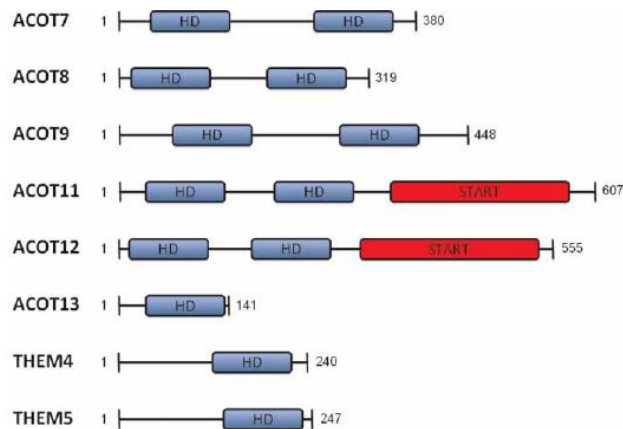


Figure 1.5 Domain organizations of human Type II acyl-CoA thioesterases (ACOTs). Closest homologues (THEM4 and THEM5) are included for comparison. HD is short for hotdog domain; START is short for steroidogenic acute regulatory protein (StAR)-related lipid transfer (START) domain; THEM is short for thioesterase superfamily member¹⁰

The Type II thioesterases, belong to the hotdog-fold thioesterase superfamily¹⁵. Although the sequence identity level is low, the conservation of fold is high in type II thioesterases (Figure 1.5). Acot7, the most well studied acyl-CoA thioesterase, exhibits a broad range of substrate specificity towards medium and long chain fatty acyl-CoA thioesters. Moreover, Acot7 is a predicted drug target for inflammatory disease due to its high expression within macrophages¹⁶. Acot8 is another peroxisomal thioesterase with the broadest range of activity toward all kinds acyl-CoA. The interaction between Acot8 and HIV-1 Nef protein has been identified¹⁷. There is not much known about Acot9 and Acot10, although they were characterized within several species. Acot11 is also known as BIFT. The mitochondrial location signal sequence was found in the N-terminal of Acot11, while the C-terminal of Acot11 is a steroidogenic acute regulatory protein-related lipid

transfer (START) domain (Figure 1.5). It has been reported that Acot11 possesses a preference for long chain acyl-CoA over shorter chain acyl-CoA¹⁸. Acot12 displays 46–50% sequence identity to Acot11. Like Acot11, Acot12 also contains a C-terminal START domain. The biological function of Acot12 has not been described yet. Chapter three of this thesis will focus on Acot12 function and structure. Acot13 was named as thioesterase superfamily member2 (THEM2). The difference between structure of Acot13 and structure of other members in type II thioesterases is that Acot13 only contains one hotdog domain instead of two. Recent studies indicate that Acot13 not only catalyzes long chain acyl-CoA but also regulates hepatic lipid and glucose metabolism¹⁹. THEM4 and THEM5 also belong to type II thioesterases. Similar to Acot13, THEM4 and THEM5 only have a single hotdog domain. THEM4, a mitochondrial protein, was verified to prefer long chain acyl-CoA²⁰. THEM5 exhibits high catalytic activity on long and unsaturated fatty acid-CoA esters²¹.

1.6 References

1. Dijkstra, M. N. a. B. W., Alpha/beta Hydrolase fold enzymes: the family keeps growing. *Current Opinion in Structural Biology* **1999**, (9), 732-737.
2. Mary C. Hunt, S. E. H. A., The role Acyl-CoA thioesterases play in mediating intracellular lipid metabolism. *Progress in Lipid Research* **2002**, 41 (99), 130.
3. Minsun Leesong, B. S. H., James R Gillig, John M Schwab and Janet L Smith, Structure of a dehydratase–isomerase from the bacterial pathway for biosynthesis of unsaturated fatty acids: two catalytic activities in one active site. *Structure* **1996**, 4 (3), 253-264.
4. Pidugu, L. S.; Maity, K.; Ramaswamy, K.; Surolia, N.; Suguna, K., Analysis of proteins with the 'hot dog' fold: prediction of function and identification of catalytic residues of hypothetical proteins. *BMC structural biology* **2009**, 9, 37.
5. Thoden, J. B.; Zhuang, Z.; Dunaway-Mariano, D.; Holden, H. M., The structure of 4-hydroxybenzoyl-CoA thioesterase from arthrobacter sp. strain SU. *The Journal of biological chemistry* **2003**, 278 (44), 43709-16.
6. Dillon, S. C.; Bateman, A., The Hotdog fold: wrapping up a superfamily of thioesterases and dehydratases. *BMC bioinformatics* **2004**, 5, 109.
7. Gerding, M. A.; Ogata, Y.; Pecora, N. D.; Niki, H.; de Boer, P. A., The trans-envelope Tol-Pal complex is part of the cell division machinery and required for proper outer-membrane invagination during cell constriction in *E. coli*. *Molecular microbiology* **2007**, 63 (4), 1008-25.
8. Kunishima, N.; Asada, Y.; Sugahara, M.; Ishijima, J.; Nodake, Y.; Miyano, M.; Kuramitsu, S.; Yokoyama, S., A novel induced-fit reaction mechanism of asymmetric hot dog thioesterase PAAI. *Journal of molecular biology* **2005**, 352 (1), 212-28.
9. Kirkby, B.; Roman, N.; Kobe, B.; Kellie, S.; Forwood, J. K., Functional and structural properties of mammalian acyl-coenzyme A thioesterases. *Prog Lipid Res* **2010**, 49 (4), 366-77.

10. Chad Brocker, C. C., Daniel W. Nebert and Vasilis Vasiliou, Evolutionary divergence and functions of the human acyl-CoA thioesterase gene (ACOT) family. *HUMAN GENOMICS* **2010**, 4 (6), 411-420.
11. Dongol, B.; Shah, Y.; Kim, I.; Gonzalez, F. J.; Hunt, M. C., The acyl-CoA thioesterase I is regulated by PPARalpha and HNF4alpha via a distal response element in the promoter. *Journal of lipid research* **2007**, 48 (8), 1781-91.
12. Isabel Neuman, P. M., Constanza Lisdero, Cecilia Colonna, Jorge Peralta, Juan Jos, Poderoso, and Ernesto J. Podest, beta-Adrenergic stimulation controls the expression of a thioesterase specific for very-long-chain fatty acids in perfused hearts. *Biochemical and Biophysical Research Communications* **2002**, 299, 135-141.
13. Westin, M. A.; Alexson, S. E.; Hunt, M. C., Molecular cloning and characterization of two mouse peroxisome proliferator-activated receptor alpha (PPARalpha)-regulated peroxisomal acyl-CoA thioesterases. *The Journal of biological chemistry* **2004**, 279 (21), 21841-8.
14. Westin, M. A.; Hunt, M. C.; Alexson, S. E., Peroxisomes contain a specific phytanoyl-CoA/pristanoyl-CoA thioesterase acting as a novel auxiliary enzyme in alpha- and beta-oxidation of methyl-branched fatty acids in mouse. *The Journal of biological chemistry* **2007**, 282 (37), 26707-16.
15. Hunt, M. C.; Siponen, M. I.; Alexson, S. E., The emerging role of acyl-CoA thioesterases and acyltransferases in regulating peroxisomal lipid metabolism. *Biochimica et biophysica acta* **2012**, 1822 (9), 1397-410.
16. Forwood, J. K.; Thakur, A. S.; Guncar, G.; Marfori, M.; Mouradov, D.; Meng, W.; Robinson, J.; Huber, T.; Kellie, S.; Martin, J. L.; Hume, D. A.; Kobe, B., Structural basis for recruitment of tandem hotdog domains in acyl-CoA thioesterase 7 and its role in inflammation. *Proceedings of the National Academy of Sciences of the United States of America* **2007**, 104 (25), 10382-7.
17. Lang Xia Liu, F. M., Sylvie Le Galli, Olivier Schwartzi, Luc Selig, Richard Benarous, and Serge Benichou, Binding of HIV-1 Nef to a Novel Thioesterase

Enzyme Correlates with Nef-mediated CD4 Down-regulation. *The Journal of biological chemistry* **1997**, 272 (21), 13779–13785.

18. Chen, D.; Latham, J.; Zhao, H.; Bisoffi, M.; Farelli, J.; Dunaway-Mariano, D., Human brown fat inducible thioesterase variant 2 cellular localization and catalytic function. *Biochemistry* **2012**, 51 (35), 6990-9.

19. Hye Won Kang, M. W. N., Shuxin Han, Yuki Kawano, and David E. Cohen, Thioesterase superfamily member 2/acyl-CoA thioesterase 13 (Them2/Acot13) regulates hepatic lipid and glucose metabolism. *the FASEB Journal* **2012**, 26 (5), 2209–2221.

20. Zhao, H.; Lim, K.; Choudry, A.; Latham, J. A.; Pathak, M. C.; Dominguez, D.; Luo, L.; Herzberg, O.; Dunaway-Mariano, D., Correlation of structure and function in the human hotdog-fold enzyme hTHEM4. *Biochemistry* **2012**, 51 (33), 6490-2.

21. Zhuravleva, E.; Gut, H.; Hynx, D.; Marcellin, D.; Bleck, C. K.; Genoud, C.; Cron, P.; Keusch, J. J.; Dummler, B.; Esposti, M. D.; Hemmings, B. A., Acyl coenzyme A thioesterase Them5/Acot15 is involved in cardiolipin remodeling and fatty liver development. *Molecular and cellular biology* **2012**, 32 (14), 2685-97.

CHAPTER TWO

CHARACTERIZATION OF THE HOTDOG FOLD THIOESTERASE

YIGI FROM *E. COLI*

2.1 Introduction

As one of the last two unknown hotdog-fold proteins from *E. coli*, studying structure-function relationships of YigI will give us a better understanding of the structural determinants for substrate recognition and thus function.

YigI, a member of 4HBT superfamily, is conserved in gamma-proteobacteria (Figure 2.1). The most frequent gene neighbors are *rarD* and *pldA*. The co-expression of these three genes was previously predicted.

The gene *pldA* encodes the enzyme phospholipase A, which cleaves the ester units in phospholipids liberating the free fatty acids^{1,2}. The free fatty acids then can undergo β -oxidation in mitochondria which leads to removal of 2-carbon units in the form of acetyl-CoA. Since *yigI* is co-expressed with *pldA*, YigI might play a housekeeper role in fatty acyl-CoA oxidation.

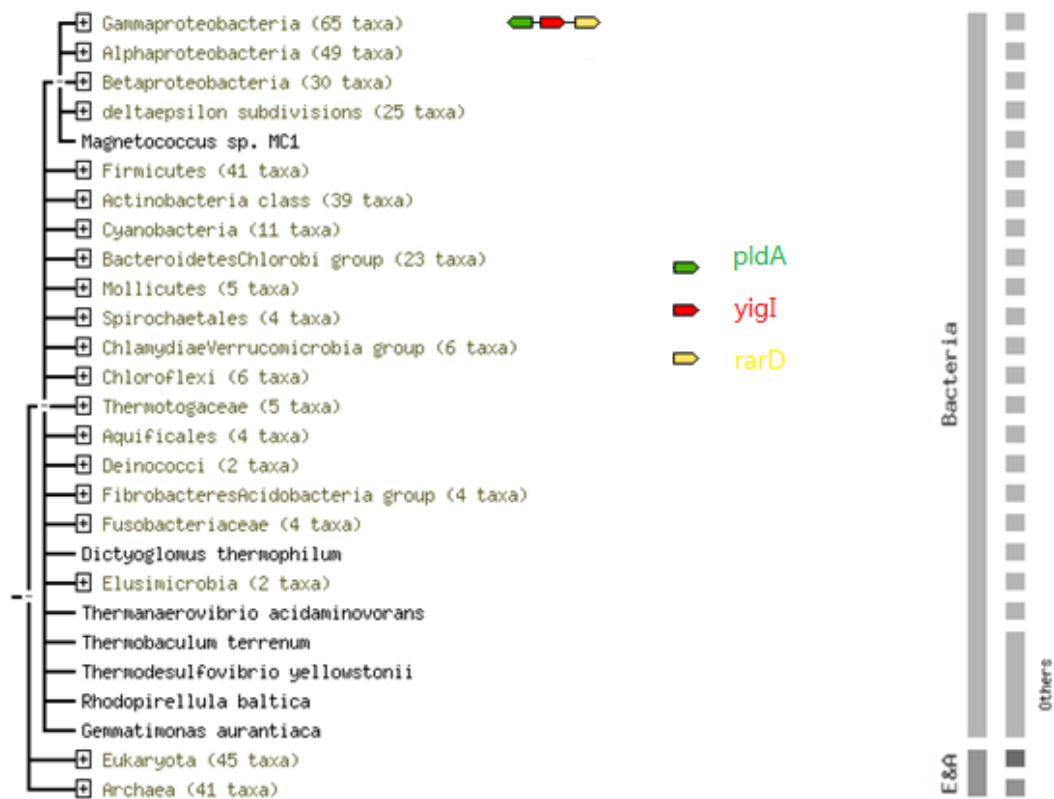


Figure 2.1 Evolutionary tree of YigI. Converted neighbor genes were shown.

2.2 Methods and Materials

2.2.1 Materials

Pfu Turbo DNA polymerase was purchased from Strategene (Santa Clara, CA). Oligonucleotide primers were custom-synthesized. T4 DNA ligase and all restriction enzymes were purchased from Invitrogen (Grand Island, NY). 2-Hydroxybenzoyl-CoA, 3-hydroxybenzoyl-CoA and 2,4-DHN-CoA were synthesized as previously reported^{3, 4}.

Hexanoyl-CoA, octanoyl-CoA, decanoyl-CoA, lauroyl-CoA, myristoyl-CoA, palmitoyl-CoA, benzoyl-CoA were purchased from Sigma.

2.2.2 Preparation of wild-type *E. coli* YigI

The wild-type *yigI* gene (UniPort #P0ADP2) was amplified through PCR using genomic DNA of *E. coli* strain K-12 (ATCC). YigI was subcloned into pET28a (Novagen) with the *NdeI* and *XhoI* restriction sites by Genscript (Piscataway, NJ). The *yigI*/pET28a plasmid was used to transform BL21 (AI) chemically competent cells (Invitrogen). The *yigI*/pET28a transformed BL21 (AI) cells were grown aerobically at 37 °C in 2L LB broth supplemented with 100 µg/mL kanamycin. When the cell culture reached an OD₆₀₀ ~ 0.6, the N-terminal His₆ tagged *yigI* protein was induced with 0.4 mM IPTG and incubated at 16 °C for 12 h. Following the induction period, the cells were harvested as described above. Purification of the His₆-*yigI* followed the procedures described above using 50 mM Bis-Tris, 50 mM imidazole, and 500 mM NaCl as lysis buffer and 50 mM Bis-Tris, 500 mM imidazole, and 500 mM NaCl as elution buffer. Yield: ~ 0.5 mg/g wet cell paste.

2.2.3 Determination of the steady state kinetic constants

The 5,5'-dithio-bis-(2-nitrobenzoic acid) (DTNB) coupled assay was used to measure the thioesterase activity. Reactions were carried out in 50 mM K⁺HEPES and 2 mM DTNB

(pH 7.5, 25 °C) containing thioesterase and varying concentrations of thioester (0.5 – 5 x K_m) in a total volume of 500 μ L and monitored at 412 nm ($\Delta\epsilon = 13.6 \text{ mM}^{-1}\cdot\text{cm}^{-1}$) using a Shimadzu UV-1800 spectrophotometer. For all measurements, the initial velocity data, measured as a function of substrate concentration, were analyzed using Enzyme Kinetics v 1.4 and equation (1).

$$V = V_{\max} [S]/([S]+K_m) \quad (1)$$

where V is initial velocity, V_{\max} is maximum velocity, $[S]$ is substrate concentration, and K_m is the Michaelis constant. The k_{cat} was calculated from $V_{\max}/[E]$ where $[E]$ is the total enzyme concentration as determined by the Bradford method.

2.2.4 Site-directed mutagenesis

Site-directed mutagenesis was carried out using the Quick Change PCR (Stratagene). WT *yigI*/pET-28 plasmid was used as template and *Pfu Turbo* is the polymerase. The mutant plasmids were confirmed through DNA sequencing before transforming into *E. coli*. BL21 (AI) competent cells (Invitrogen). Followed the same procedure with purification of wild type YigI, the mutant proteins were purified and confirmed by ES-MS.

2.2.5 Molecular mass determination

Fractions containing the His₆-yigI were applied to a HiPrep 16/60 Sephacryl S-200 HR (GE Life Sciences) size exclusion column attached to a FPLC (AKTA) using 50 mM Bis-Tris, 500 mM NaCl as the mobile phase. The His₆-yigI eluted as a monomer at ~58 mL having a calculated molecular weight of ~38 kDa.

2.3 Results and discussion

2.3.1 Recombinant yigI purification and verification

Wild-type recombinant YigI (UniProt accession code P0ADP2) was prepared as described in Materials and Methods. The subunit molecular weight determined by SDS-PAGE is ~20 kDa (Figure 2.2).

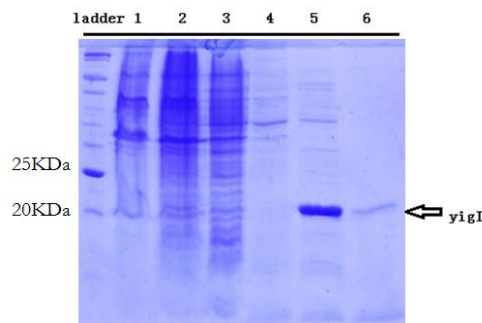


Figure 2.2 Molecular weight determined by SDS-page. 1, centrifuge cell precipitant after French press; 2, cell lysis before centrifuge (whole cell) 3, centrifuge cell supernatant after French press; 4, 5, 6, are different fractions from the Ni column chromatography.

The subunit molecular weight of His₆-tagged YigI subunit determined by ES-MS (Figure 2.3) is 19194.4.

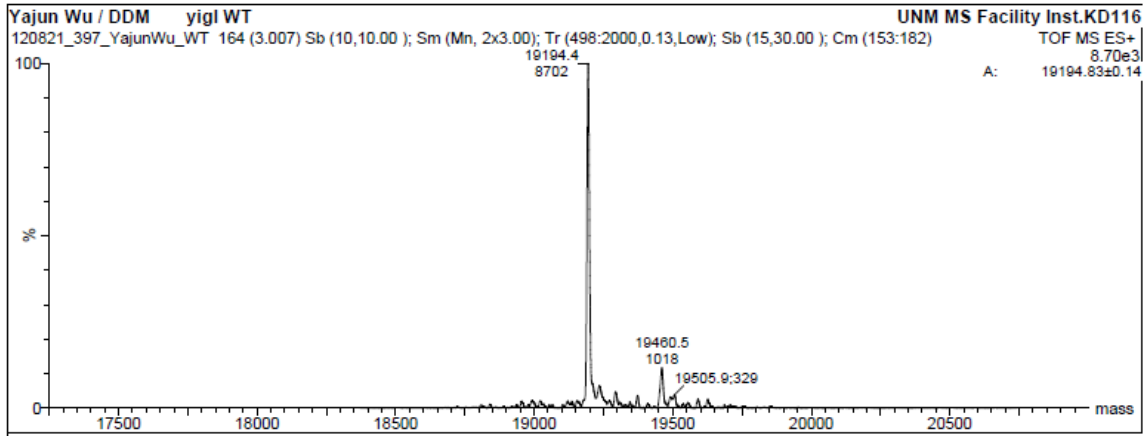


Figure 2.3 Molecular weight determined by Mass Spectrometer.

Compared to the theoretical molecular weight calculated from EXPASY 19194.9, the molecular weight measured by experiment is close enough to conclude that YigI was successfully purified.

The functional quaternary structure of the hotdog fold thioesterase is either a dimer or a dimer of dimer (tetramer). FPLC size exclusion chromatography indicates that YigI is a dimer of dimer (tetramer). As shown in Figure 2.4, native YigI eluted at 55.8 mL, which corresponds to a native molecular weight is ~84 kDa, compared to the calculated molecular weight of the tetramer of 77 kDa.

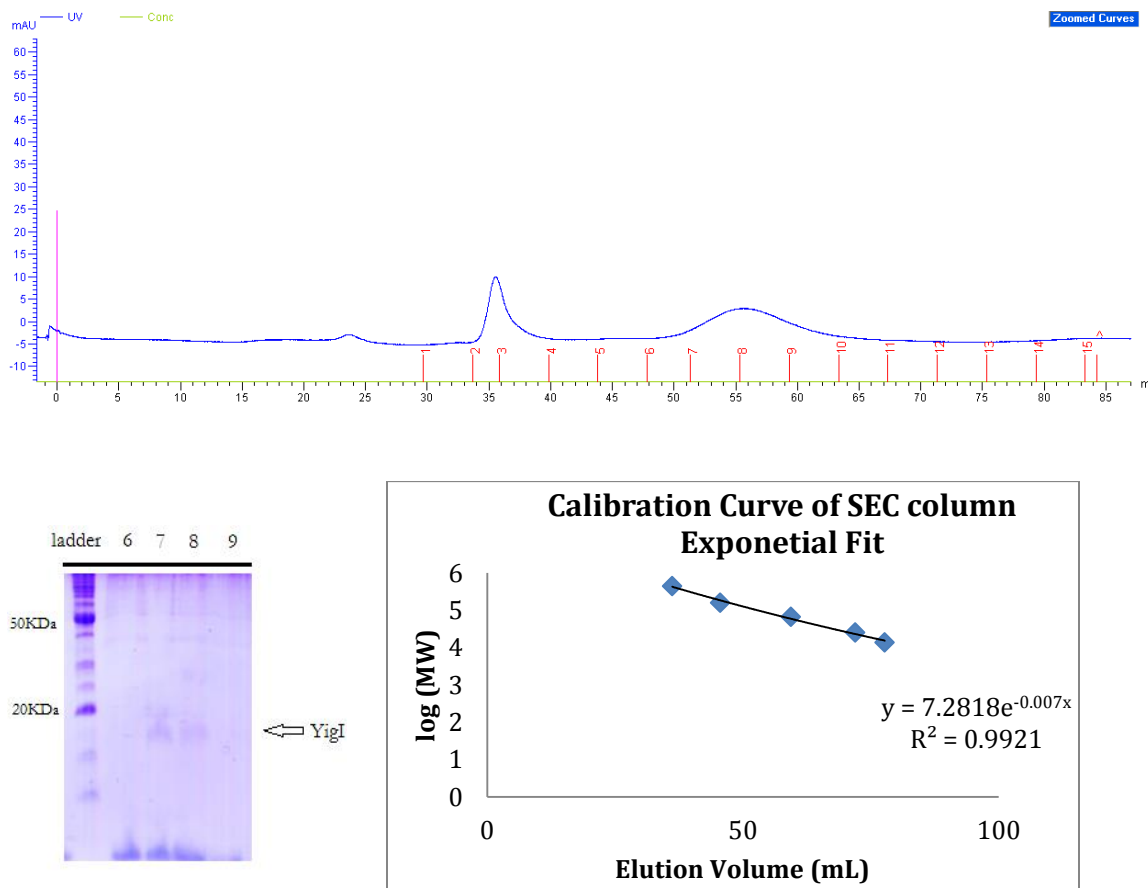


Figure 2.4 (top) FPLC size exclusion chromatography elution profile, (bottom left) SDS-PAGE of fractions 6, 7, 8 and 9, and (bottom right) calibration plot using protein molecular weight standards.

2.3.2 YigI substrate specificity profile determination

By measuring steady-state kinetic constants k_{cat} and K_m for different coenzyme A thioesters (Figure 2.5), the YigI substrate specificity profile was determined (Table 2.1; Figure 2.6). For the fatty-acyl CoA substrates, the k_{cat}/K_m values increased with increasing chain length. The polar acyl-CoA thioester succinyl-CoA was not a substrate.

Likewise, the benzoyl-, chlorobenzoyl-, 4 or 3-hydroxybenzoyl- and 2,4-dihydroxynaphthoyl-CoA thioesters are not substrates.

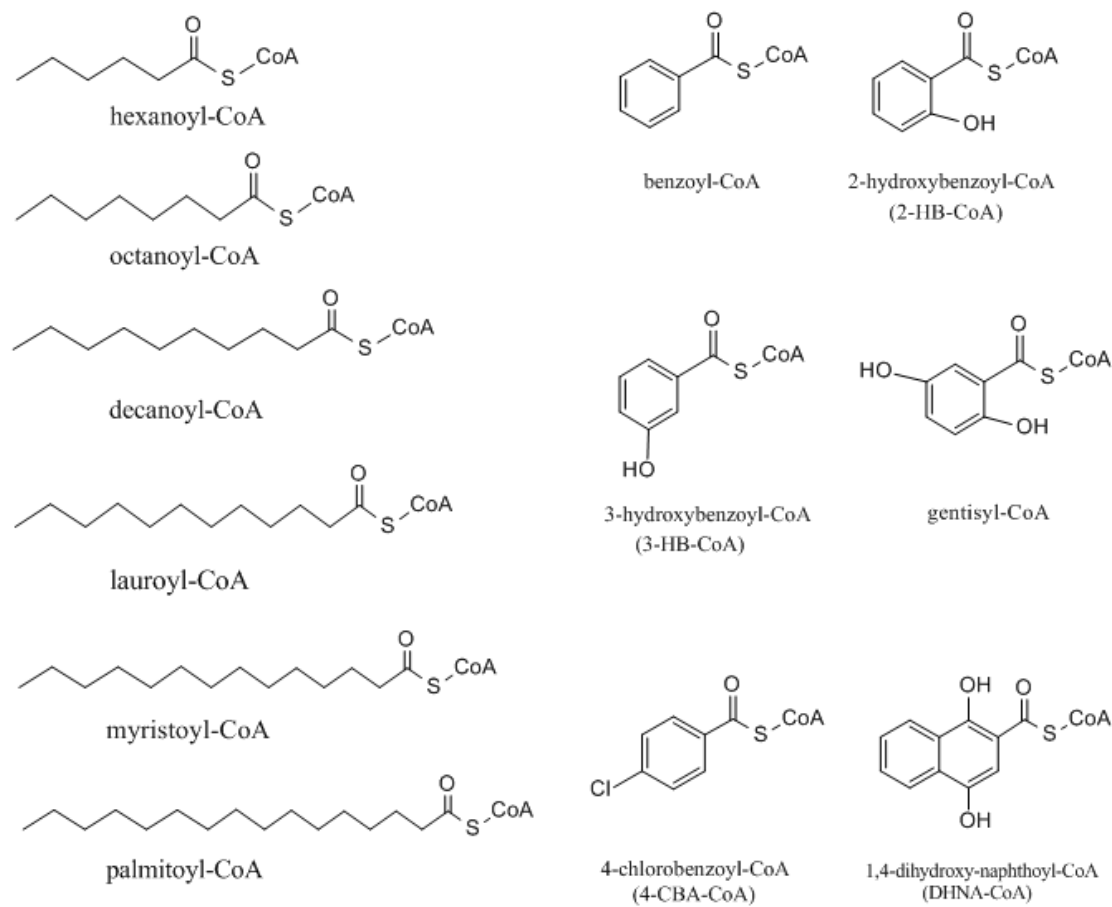


Figure 2.5 The molecular structure of selected acyl/aryl-coenzyme compounds for the YigI substrate screening.

In order to determine if the inactivity of the aromatic thioesters was the result of low binding affinity, benzoyl-CoA was tested as a competitive inhibitor of YigI-catalyzed hydrolysis of 18 μ M decanoyl-CoA (pH 7.5, 25 $^{\circ}$ C, DTNB assay). No inhibition was

observed at a benzoyl-CoA concentration of 1 mM thus suggesting that YigI does not bind the benzoyl-CoA with significant affinity.

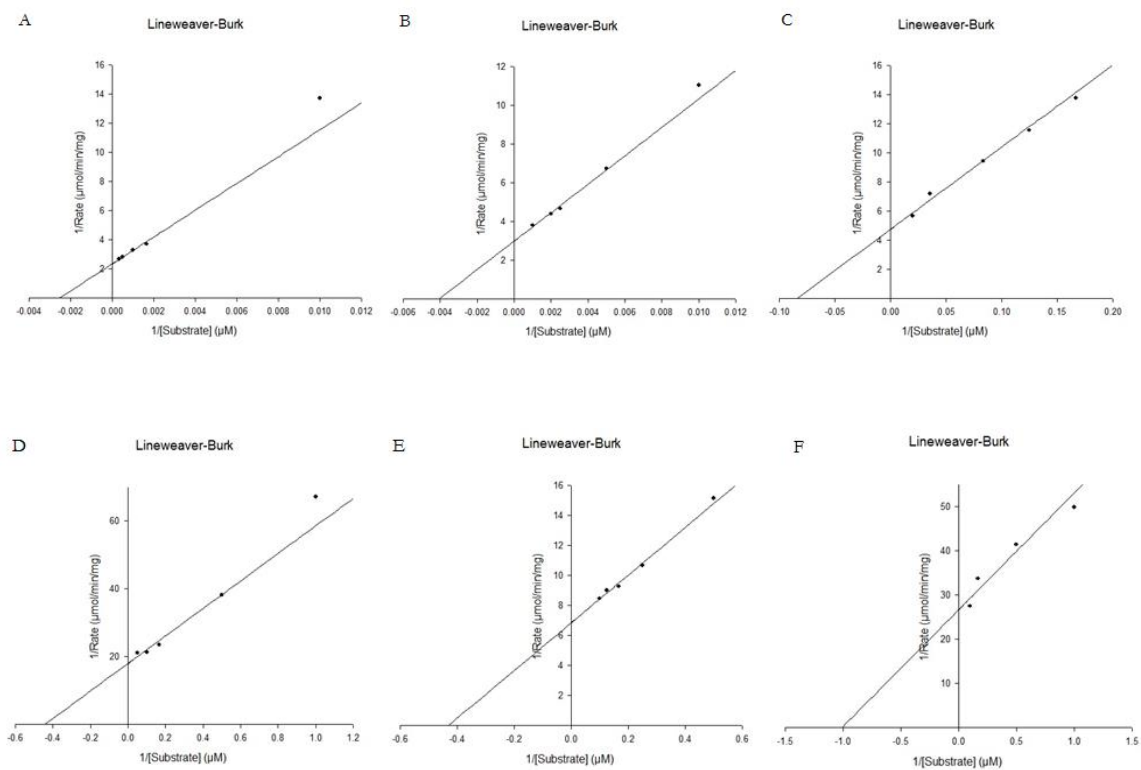


Figure 2.6 Lineweaver Burk plots measured for YigI-catalyzed hydrolysis of (A) hexanoyl-CoA, (B) octanoyl-CoA, (C) decanoyl-CoA, (D) lauroyl-CoA (E) myristoyl-CoA and (F) palmitoyl-CoA. See Materials and Methods for details

YigI Thioesterase			
Substrate	k_{cat} (s^{-1})	K_M (μM)	k_{cat}/K_M ($M^{-1}s^{-1}$)
hexanoyl-CoA	0.78 \pm 0.01	548 \pm 52	1.4 x 10 ³
octanoyl-CoA	0.76 \pm 0.01	263 \pm 26	2.9 x 10 ³
decanoyl-CoA	1.18 \pm 0.05	17 \pm 0.4	6.9 x 10 ⁴
lauroyl-CoA	(1.54 \pm 0.03)x 10 ⁻¹	3.0 \pm 0.3	5.1 x 10 ⁴
myristoyl-CoA	(4.56 \pm 0.05)x 10 ⁻¹	2.3 \pm 0.2	2.0 x 10 ⁵
palmitoyl-CoA	(9.3 \pm 0.9) x 10 ⁻²	1.0 \pm 0.1	9.3 x10 ⁴
succinyl-CoA	N/A		
benzoyl-CoA	N/A		
2-HB-CoA	N/A		
3-HB-CoA	N/A		
gentisyl-CoA	N/A		
2,4-DHN-CoA	N/A		
4-CB-CoA	N/A		

Table 2.1 Steady-state kinetic constants measured for YigI-catalyzed hydrolysis of various acyl-CoA substrates monitored by DTNB coupled reaction in 50 mM HEPES at pH 7.5 and 25 °C. N/A is “no detectable activity” ($k_{cat} < 1 \times 10^{-4} s^{-1}$).

2.3.3 Site-directed mutagenesis

2.3.3.1 *YigI* Structure

The *YigI* sequence was submitted to Phyre2 in order to identify the closest homolog having a known structure. The uncharacterized tetrameric type AB thioesterase from *Shewanella oneidensis* (UniProt accession code Q8E9M7) (45 % sequence identity) was identified as the closest homolog (Figure 2.7). The fold of the *S. oneidensis* monomer is compared with the folds of the monomers of *E. coli* hotdog thioesterases in Figure 2.8.

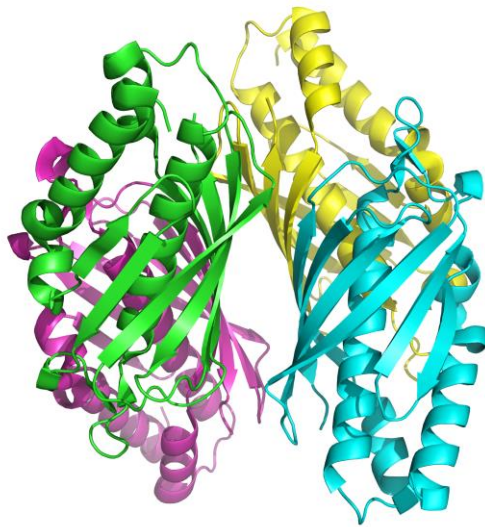


Figure 2.7 *YigI* homolog from *Shewanella oneidensis* (PDB accession code 3E8P). The yellow and cyan colored subunits form one dimer and the green and magenta colored subunits for the other dimer. The two dimers are arranged back-to-back (sheet-to-sheet) to form the tetramer.

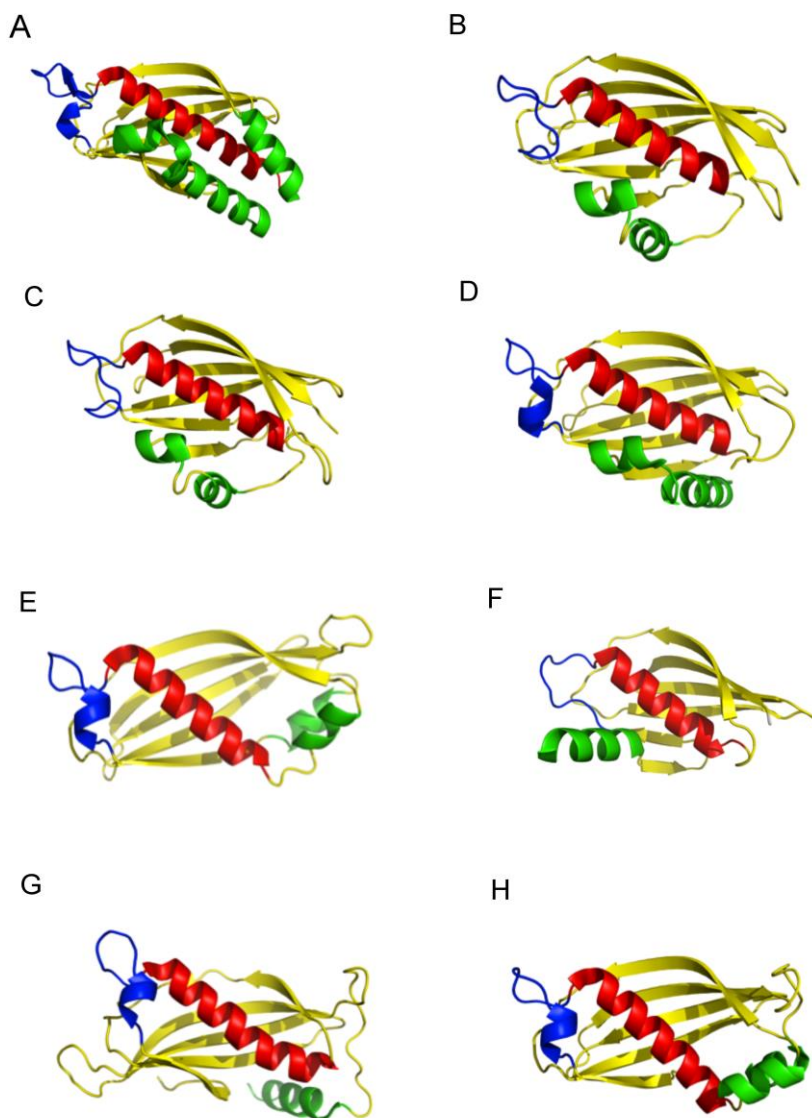


Figure 2.8 A. *S. oneidensis* (PDB accession code 3E8P) YigI homolog (type AB). B. YdiI (type AB) (PDB accession code 1VI8), C. Ybdb (type AB) (PDB accession code 1VH9), D. PaaI (type AB) (PDB accession code 2FS2), E. YbaW (Type AA) (PDB accession code 1NJK), F. YbgC (type AA) (PDB accession code 1S5U), G. Haemophilus influenza YciA homolog (type AB)(PDB accession code 1YLI), H. Double hotdog TesB (TEII) N-terminal catalytic domain (type AB) (PDB accession code 1YLI)

The monomer of the YigI homolog from *S. oneidensis* (PDB accession code 3E8P) is compared in Figure 2.8 to those of the other known thioesterases from *E. coli*.

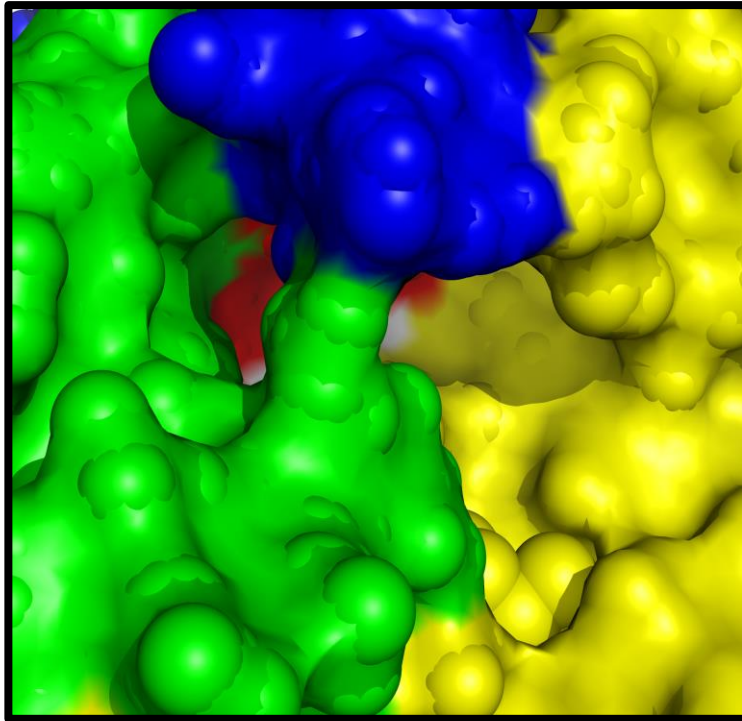


Figure 2.9 Surface representations of the *S. oneidensis* (PDB accession code 3E8P) YigI homolog tetramer. Coloring is the same as that used in Figure 2.8. The catalytic Asp is colored white, the channel on the right (yellow) is the pantethine binding site and the channel to the left (red, green and blue) is the site where the aliphatic tail is expected to bind.

For each monomer, the 5-6 stranded anti-parallel β -sheet core is colored yellow, the central α -helix is colored red, the loop leading into the N-terminus of the central α -helix

is colored blue and the additional helical segments located at the protein N- or C-terminus are colored green. The structure of the *S. oneidensis* (PDB accession code 3E8P) YigI homolog (Figure 2.8A) (and hence *E. coli* YigI) is unique in that it possess three aligned α -helices which form the binding site for the aliphatic chain of the fatty acyl-CoA substrate: the elongated N-terminal α -helix, the long central α -helix and the shorter α -helix that extends from the central helix (see Figure 2.9).

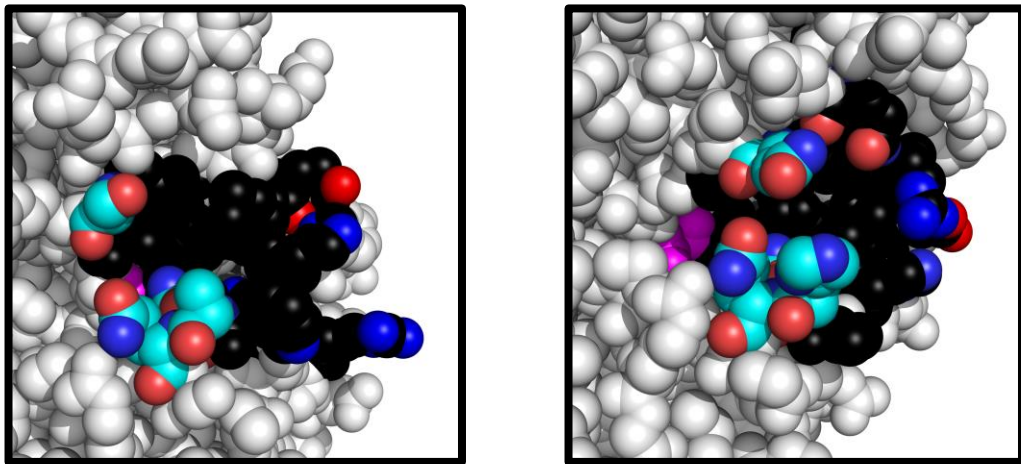


Figure 2.10 The residues that line the walls of the aliphatic tail binding pocket in the modeled *E. coli* YigI (left panel) and in the structure of the *S. oneidensis* (PDB accession code 3E8P) YigI homolog (right panel). Carbon atoms are colored black, oxygen red and nitrogen blue. The catalytic Asp is colored magenta. The carbon atoms of the three residues that form the bridge over the pocket are colored cyan.

The channel that accommodates the aliphatic tail is largely nonpolar, however the surface residues that outline the channel are polar (see Figure 2.10). The three residues that form the bridge over the channel are Gln96, Gln55 and His54 in the *S. oneidensis* YigI homolog. The counter parts in the *E. coli* YigI are Ser97, Gln56 and Ala55.

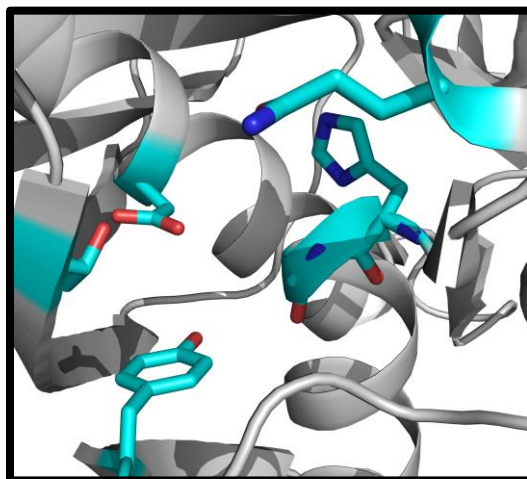


Figure 2.11 The catalytic site of the *S. oneidensis* (PDB accession code 3E8P) YigI homolog. The Asp68, Thr100, Tyr107, Asn55, Gly60 and His59 residues are shown in stick and the carbon atoms are colored cyan, oxygen atoms red and nitrogen atoms blue.

The residues that form the catalytic site in the *S. oneidensis* YigI homolog: Asp68, Thr100, Tyr107, Gly60 and His59 are illustrated in Figure 2.11. These residues are conserved in the *E. coli* YigI. The Asp68 residue is expected to function in nucleophilic or base catalysis and the Thr107 side chain is positioned to orient the Asp68. In the absence of liganded structure it is unclear whether it is the backbone amide NH of

Gly60 or His59 which forms a hydrogen bond with the substrate thioester C=O oxygen atom, thereby activating the carbon for nucleophilic attack. Likewise, it is not possible to predict what role, if any Gln55 and Tyr107 play in catalysis.

2.3.3 Site-directed mutagenesis

2.3.3.1 Mutant preparation and verification

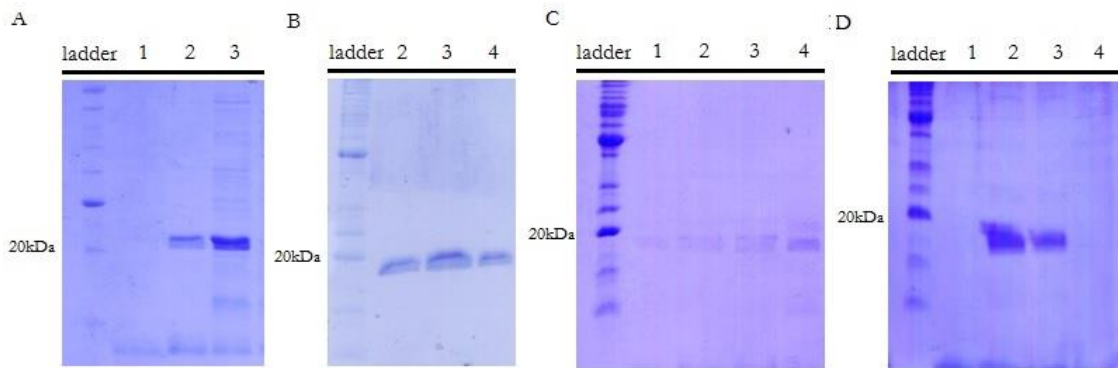


Figure 2.12 SDS-PAGE gel analyses of the YigI mutants containing fractions (A) D69Q, (B) Q56A, (C) H60A, (D) D69E pictured in the gel stained with Coomassie blue dye. See Materials and Methods for details

In order to determine the contributions that the catalytic site residues identified in the previous section make to the catalytic efficiency site-directed mutants were prepared for steady-state kinetic constant determination. The residues targeted are *E. coli* YgiI Asp69, Gln56 and His60. The mutants were prepared by using a PCR-based strategy, and

purified to homogeneity using a His6-tag Ni affinity column (SDS-PAGE gels are shown in Figure 2.12). The yields of the mutant proteins in mg protein per g of wet cells are as follows: D69Q ~0.2 mg/g, D69E ~0.2 mg/g, Q56A ~0.2 mg/g, H60A ~0.2 mg/g. The identity of each mutant protein was verified by ES-MS: D69Q (calculated 19207.9 Da; found 19208.0 Da), D69E (calculated 19208.9 Da; found 19209.2 Da), Q56A (calculated mass 19137.9Da; found 19138.1Da) and H60A (calculated mass 19128.9 Da; found 19128.6 Da)

2.3.3.3 *YigI* mutants kinetic constants

YigI Thioesterase			
Mutants	k_{cat} (s⁻¹)	K_M (μM)	k_{cat}/K_M(M⁻¹s⁻¹)
WT	(4.56±0.05)x 10 ⁻¹	2.3±0.2	2.0 x 10 ⁵
H60A	(2.02±0.01)x 10 ⁻¹	2.2±0.2	9.2 x 10 ⁴
D69Q	N/A		
D69E	N/A		
Q56A	N/A		

Table 2.2 Steady state kinetics study of YigI mutant-catalyzed hydrolysis of myristoyl-CoA at pH 7.5 and 25 °C. N/A is “no detectable activity” ($k_{cat} < 1 \times 10^{-4} \text{ s}^{-1}$).

The steady-state kinetics constants of wild-type and mutant *E. coli* YigI-catalyzed hydrolysis of myristoyl-CoA were measured and are reported in Table 2.2. YigI D69Q and D69E were found to be completely inactive, suggesting Asp69 is an important catalytic residue. Likewise, the Gln56Ala mutant was catalytically inactive. The k_{cat} value of the H60A mutant is reduced by two-fold and the $k_{\text{cat}}/K_{\text{m}}$ value is decreased by ten-fold.

2.3.4 Conclusion

Based on the substrate specificity profile analysis the likely function of YigI is the hydrolysis of fatty acyl-CoA thioesters. The preference for substrates that liberate fatty acids that are most prevalent in the cellular membrane phospholipids suggests that YigI is important to membrane biogenesis. YigI is one of the eight hotdog-fold thioesterases in *E. coli*. Six of these, among them YigI belong to the type AB clade and the other two to the type AA clade.

2.4 References

1. Hiroshi Homma, T. K., Nobuyoshi Chiba, Ken Karasawa, Hiroshi Mizushima, Ichiro Kudo, Keizo Inoue, Hideo Ikeda, Mutsuo Sekiguchi, and Shoshichi Nojima, The DNA sequence encoding pldA gene, the structural gene for detergent-resistant phospholipase A of *E. coli*. *J. Biochem* **1984**, *96*, 1655-1664.
2. Kathleen A. Grant, I. U. B., Niek Dekker, Peter T. Richardson, AND Simon F. Park, Molecular characterization of pldA, the structural gene for a phospholipase A from *Campylobacter coli*, and its contribution to cell-associated hemolysis. *INFECTION AND IMMUNITY* **1997**, *65* (4), 1172–1180.
3. Zu-Feng Guo, Y. S., Suilan Zheng, and Zhihong Guo, preferential hydrolysis of aberrant intermediates by the type II thioesterase in *Escherichia coli* nonribosomal enterobactin synthesis: substrate specificities and mutagenic studies on the active-site residues. *Biochemistry* **2009**, *48*, 1712–1722.
4. Susan M. Merkel, A. E. E., Jane Gibson, AND Caroline S. Harwood, Involvement of coenzyme A thioesters in anaerobic metabolism of 4-hydroxybenzoate by *Rhodospirillum rubrum*. *JOURNAL OF BACTERIOLOGY* **1989**, *171* (1), 1-7.

CHAPTER THREE

DETERMINATION THE FUNCTION OF HOTDOG-FOLD THIOESTERASES “CYTOPLASMIC ACETYL-COENZYME A HYDROLASE” (CACH) FROM HUMAN

3.1 Introduction

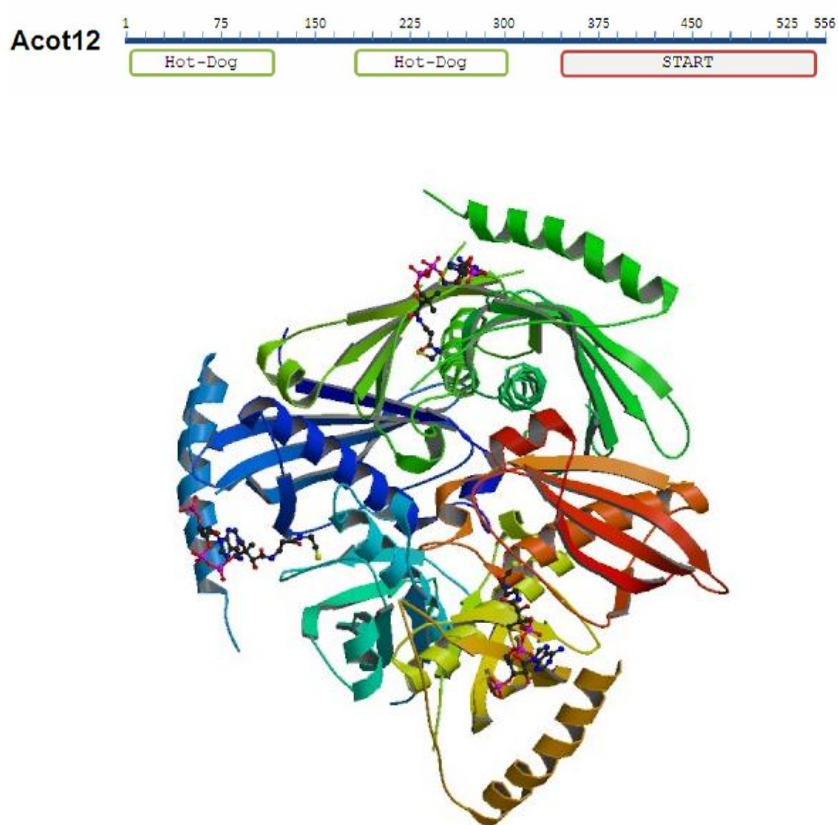


Figure 3.1 Domain organizations (top) and crystal structure (bottom) (PDB ID: 3B7K) of Acot12¹.

Acot12, also known as cytoplasmic acetyl-coenzyme A hydrolase (CACH), is a multidomain Type-II thioesterase (Figure 3.1). The N-terminal double hotdog-fold domain unit (two tandem hotdog-fold domains) is fused to C-terminal START domain (Stard 15)².

Acot12 displays 46–50% sequence identity to Acot11 (otherwise known as BFIT). Both thioesterases are structurally unrelated to the α,β -hydrolase fold “Type-I thioesterases”. Previous studies have shown that the high expression of Acot12 was found in proximal intestinal epithelium, liver and kidney³. This indicates Acot12 may play an important role in lipid metabolism.

The structure for the double hotdog domain unit of Acot12 (CACH) was deposited in the PDB (PDB ID: 3B7K) in 2008. However, the analysis of the structure with ligand has not been published. Also, there is no in-depth kinetic characterization of CACH. Therefore, Chapter three will focus on the structure and function of CACH.

3.2 Materials and Methods

3.2.1 Materials

CACH (residues 7-310) domains were codon optimized for *E. coli* and subcloned into pET28a with the NdeI and XhoI restriction sites by Genscript (Piscataway, NJ). The PIP Arrays, PIP Strips, and Membrane Lipid Strips were purchased from Echelon (Salt Lake City, UT). The anti-ACOT12 (216-265) was purchased from Abcam

(Cambridge, MA) and anti-ACOT12 (456-470) was purchased from Sigma Aldrich (St. Louis, MO). The anti-rabbit HRP was purchased from Santa Cruz Biotechnology (Santa Cruz, CA). The Pierce Direct IP Kit was purchased from Thermo Scientific (Waltham, MA). All other reagents were purchased from Sigma Aldrich unless otherwise stated.

3.2.2 Expression and purification of CACH

The CACH/pET28a plasmid was used to transform BL21 (DE3) chemically competent cells (Invitrogen). The CACH/pET28a transformed BL21 (DE3) cells were grown aerobically at 37 °C in 1.5 L TB broth supplemented with 8g/L glycerol and 100 µg/mL kanamycin. When the cell culture reached an OD600 ~ 1.2, the N-terminal His6- γ tagged CACH protein was induced with 0.4 mM IPTG and incubated at 16 °C for 12 h. Following the induction period, the cells were harvested as described above. Purification of the His6-CACH followed the procedures described above using 20 mM NaH₂PO₄, 40 mM Na₂HPO₄, 50 mM imidazole, 500 mM NaCl, and 10% glycerol as lysis buffer and 20 mM NaH₂PO₄, 40 mM Na₂HPO₄, 500 mM imidazole, 500 mM NaCl, and 10% glycerol as elution buffer. Fractions containing the His6-CACH were applied to a HiPrep 16/60 Sephacryl S-200 HR (GE Life Sciences) size exclusion column attached to a FPLC (AKTA) using 20 mM NaH₂PO₄, 40 mM Na₂HPO₄, 50 mM NaCl, 10% glycerol as the mobile phase. The His6-CACH eluted as a monomer at ~62 mL having a calculated molecular weight of ~37 kDa. Yield: ~ 0.5 mg/g wet cell paste.

3.2.3 Steady-state kinetic analysis of CACH.

Thioesterase activity was measured using the 5,5'-dithio-bis-(2-nitrobenzoic acid) (DTNB) coupled assay. Reactions were monitored at 412 nm ($\Delta\epsilon = 13.6 \text{ mM}^{-1}\cdot\text{cm}^{-1}$) using a Shimadzu UV-1800 spectrophotometer. Reactions were carried out in 50 mM K+HEPES and 1 mM DTNB (pH 7.5, 25 °C) containing thioesterase and varying concentrations of thioester ($0.5 - 5 \times K_m$) in a total volume of 500 μL . For all measurements, the initial velocity data, measured as a function of substrate concentration, were analyzed using Enzyme Kinetics v 1.4 and equation (1).

$$V = V_{\max} [S]/([S]+K_m) \quad (1)$$

where V is initial velocity, V max is maximum velocity, [S] is substrate concentration, and Km is the Michaelis constant. The k_{cat} was calculated from $V_{\max}/[E]$ where [E] is the total enzyme concentration as determined by the Bradford method.

3.2.4 Protein-Lipid Overlay Assay

Each PIP Array, PIP Strip or Membrane Lipid Strip was blocked with PBS containing 0.1% Tween (PBS-T) and 3% BSA for 1 h prior to being incubated with 0.5 $\mu\text{g}/\text{mL}$ StarD15 or 0.5 $\mu\text{g}/\text{mL}$ CACH for 1 hour at room temperature. After 1 wash for 15 min and 3 washes for 5 min with PBS-T buffer, each strip or array was incubated with anti-ACOT12 (456-470) (1:1000) or anti-ACOT12 (216-256) (1:1000) at room temperature for 1 h and incubated with anti-Rabbit IgG-HRP (1:10,000) at room

temperature. The protein-lipid complex was visualized using Western Lighting Chemiluminescent Reagent Kit (PerkinElmer) and a BioRad GelDoc XR+ with the accompanying software.

3.2.5 Co-immunoprecipitation of recombinant StarD15 and CACH

Anti-ACOT12 (147-160) (anti-CACH) antibody covalently immobilized agarose beads were prepared following the manufacturer's instructions (Pierce Direct IP Kit, ThermoScientific). In short, 20 μg of the anti-CACH antibody was incubated with 40 μL of the agarose bead slurry in the presence of NaCNBH_3 at room temperature for at least 2 h. The uncoupled antibody was removed by extensive washing with wash buffer and the uncoupled reactive sites in agarose beads were quenched by incubation with the primary amine and NaCNBH_3 . Purified recombinant CACH (150 μg) and StarD15 (100 μg) dialyzed against 50 mM HEPES and 100 mM NaCl were incubated with the anti-CACH antibody immobilized agarose beads in 500 μL of IP lysis buffer at 4 $^\circ\text{C}$ for 12 h. As a control, the same amount of StarD15 was incubated with the anti-CACH antibody immobilized agarose beads in the absence of CACH. Unbound or weakly bound protein was removed by using washing steps prior to eluting the specifically bound protein from the beads with the elution buffer (10 mM Tris with 100 mM glycine pH 7.4). Protein samples were separated by SDS-PAGE before being transferred to a nitrocellulose membrane, which was then incubated for 1 h with the anti-CACH or anti-ACOT12 (456-470) (anti-StarD15) antibody at room temperature. After extensive washing, the membrane was treated with anti-rabbit-HRP antibody (Santa Cruz Biotechnology). Chemiluminescence was carried out as described above.

3.3 Results and discussion

3.3.1 CACH purification and verification

Wild-type CACH (double hotdog fold domain unit only) was purified as described above.

The molecular weight was determined by SDS-page, which is 37 kDa (Figure 3.2).

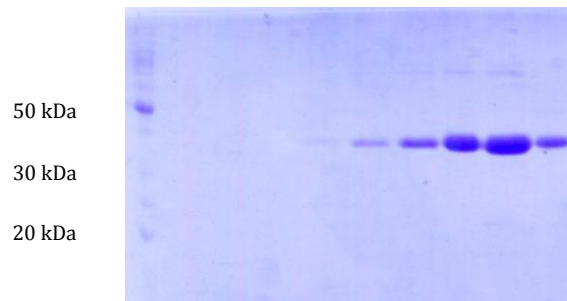


Figure 3.2 SDS-PAGE gel analysis of the CACH containing fractions pictured in the gel stained with Coomassie blue dye.

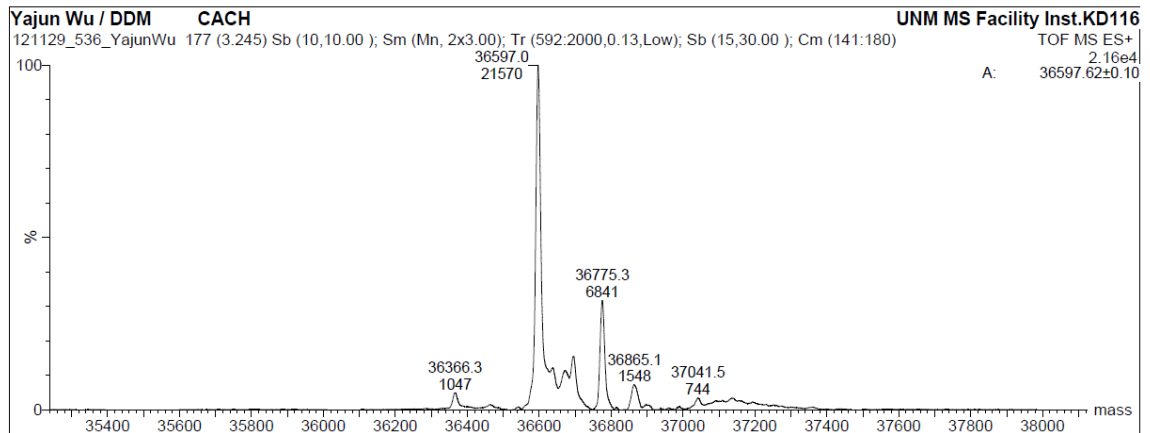


Figure 3.3 Molecular weight determined by Mass Spectrometer

The subunit molecular weight of His₆-tagged CACH subunit determined by ES-MS (Figure 3.3) is 36597.0 Da vs calculated: 36597.6 Da.

3.3.2 CACH substrate screen for determination of biochemical function

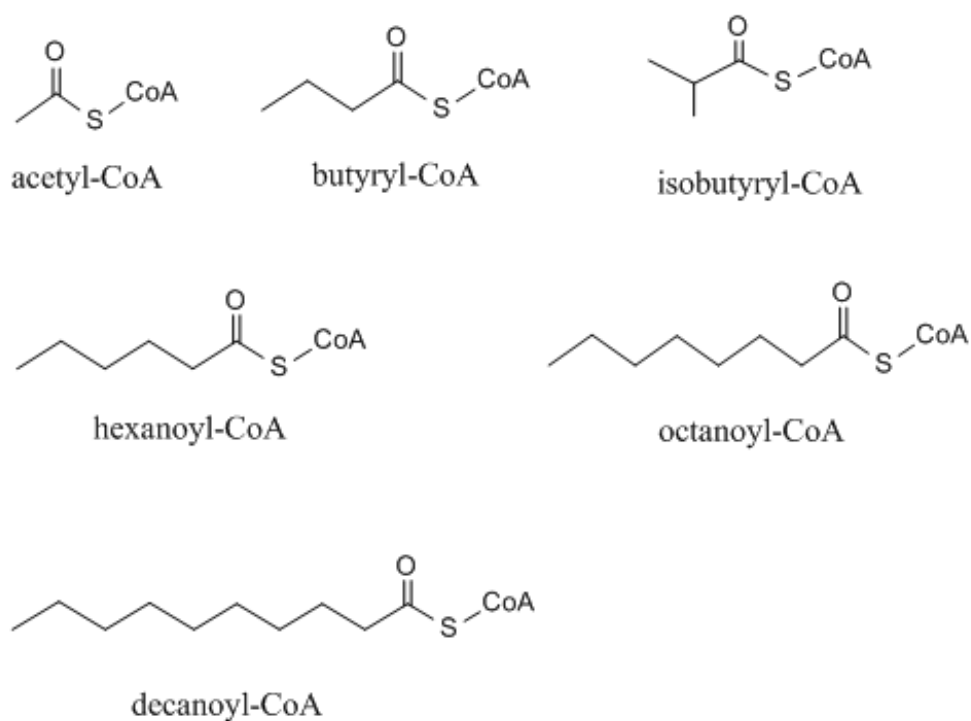


Figure 3.4 The molecular structure of selected acyl/aryl-coenzyme compounds for the CACH substrate screening.

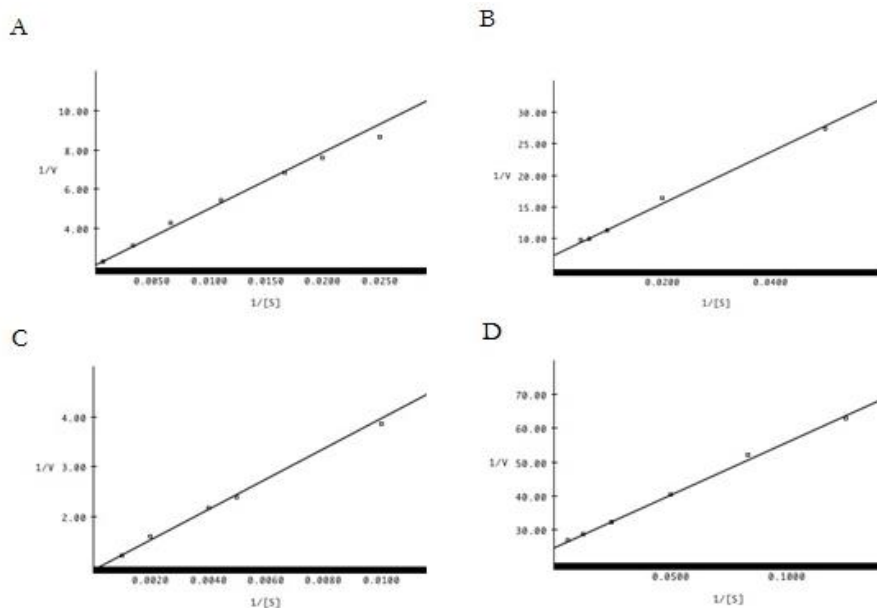


Figure 3.5 Lineweaver Burk plots measured for CACH-catalyzed hydrolysis of (A) butyryl-CoA, (B) isobutyryl-CoA, (C) hexanoyl-CoA, (D) octanoyl-CoA. See Materials and Methods for details

By measuring steady-state kinetic constants k_{cat} and K_m for different coenzyme A thioesters (Figure 3.4), the CACH substrate specificity profile was determined (Table 3.1; Figure 3.5). Unlike YigI, K_m and K_{cat}/K_m value of CACH is not correlated with the chain length of substrates. Also, not like what is predicted in previous publications¹, CACH is not active with acetyl-CoA serving as substrate. Instead, catalysis of isobutyryl-CoA has small K_m and large k_{cat}/K_m value, suggesting isobutyryl-CoA is the best substrate among all the coenzyme A tested. For decanoyl-CoA, the K_m is ~ 1.7 mM while k_{cat} is below $0.02S^{-1}$, which gives a very low K_{cat}/K_m . Thus, the kinetic constants were not determined although it is a substrate.

Substrate	k_{cat} (s^{-1})	K_M (μM)	k_{cat}/K_M ($M^{-1}s^{-1}$)
acetyl-CoA	N/A		
butyryl-CoA	$(12.10 \pm 0.08) \times 10^{-1}$	134.4 ± 6.6	8×10^3
isobutyryl-CoA	$(12.41 \pm 0.06) \times 10^{-1}$	56.3 ± 7.4	2.2×10^4
hexanoyl-CoA	$(24.43 \pm 0.05) \times 10^{-1}$	282.9 ± 44.5	8.6×10^3
octanoyl-CoA	$(1.24 \pm 0.03) \times 10^{-1}$	12.9 ± 0.4	9.6×10^3
decanoyl-CoA	$\sim 1 \times 10^{-2}$	~ 17000	

Table 3.1 Steady-state kinetic constants for CACH catalyzed hydrolysis of acyl-CoA was measured using the DTNB spectrophotometric assay at pH 7.5 and 25 °C. N/A no activity ($k_{cat} < 1 \times 10^{-4} s^{-1}$).

3.3.3 Interaction with lipids

The protein-lipid assay was carried out as described above. There is no interaction between CACH and lipids (Figure 3.6). Thus, the two hotdog domain may only function in catalysis of acyl-CoA.

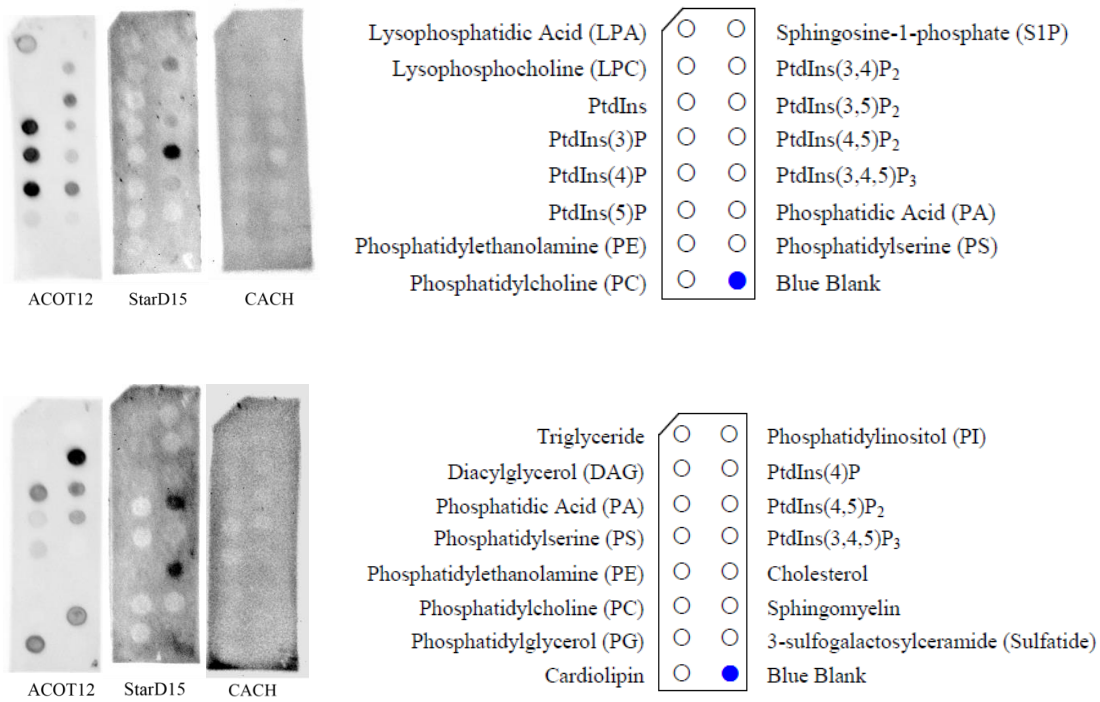


Figure 3.6 Protein–lipid overlay assays in which PIP Strips or Membrane Lipid Strips were separately treated with 2 $\mu\text{g}/\text{mL}$ ACOT12, 1 $\mu\text{g}/\text{mL}$ StarD15 domain or 1 $\mu\text{g}/\text{mL}$ CACH domain (purified as described above), in PBS-T and then imaged. The lipid positions are identified in the key. (Acot12 and StarD15, Latham, unpublished data)

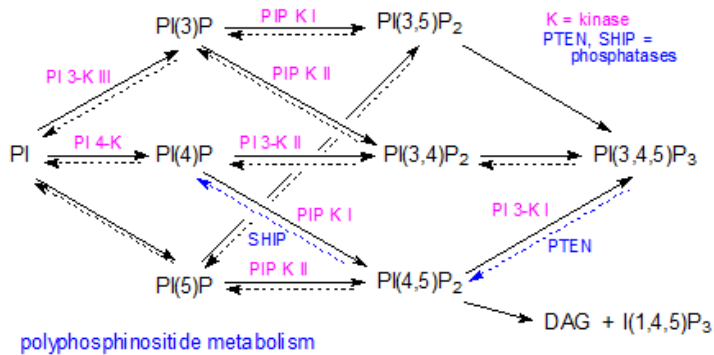


Figure 3.7 polyphosphoinositide metabolism

In contrast when the interaction between StarD15/Acot12 and lipids was tested the results were interesting. Strong interaction was observed between StarD15 and PtdIns(3,4,5)P₃ (PIP₃) or sphingomyelin (SM). While Acot12, full length CACH, presents a broad range of binding efficiency.

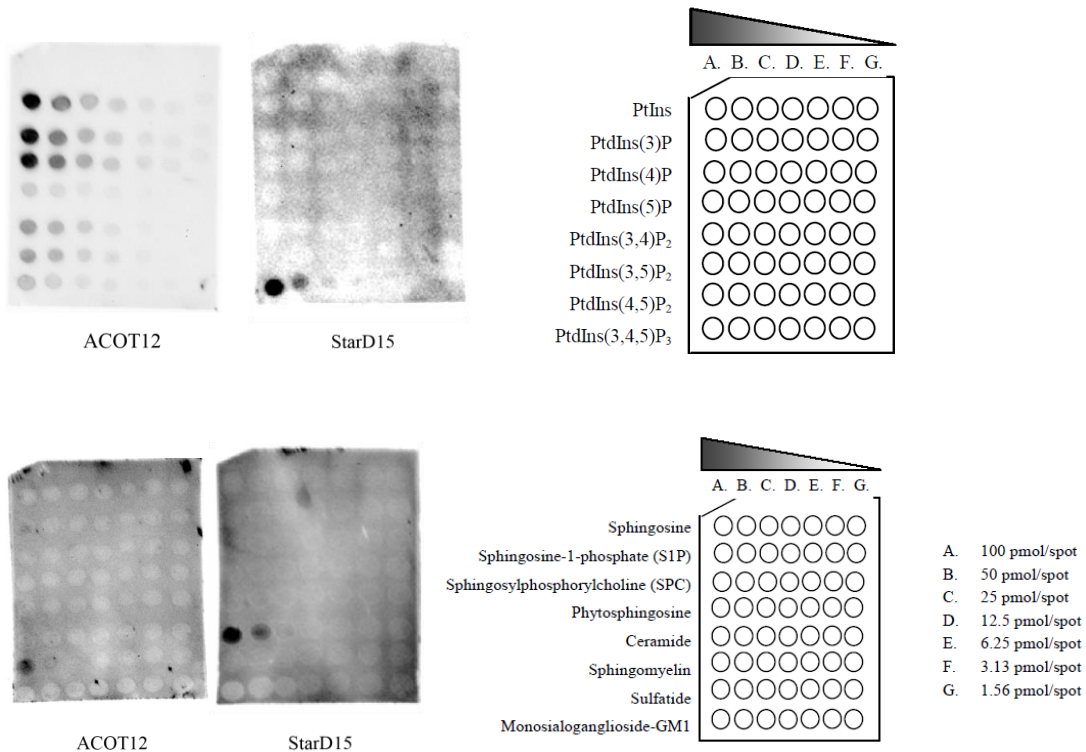


Figure 3.8 Protein–lipid overlay assays in which PIP Arrays or Sphingo Arrays (Echelon Bioscience Inc.) were separately treated with 2 $\mu\text{g}/\mu\text{L}$ ACOT12 or 1 $\mu\text{g}/\text{mL}$ StarD15 (purified as described above), in PBS-T and then imaged. The lipid positions are identified in the key. (Latham, unpublished data)

PI, PI(3)P, PI(4)P, PI(5)P, PI(3,4)P, PI(4,5)P and PI(3,4,5)P are plasma-membrane lipids⁴. The relationship among different kind of phosphatidylinositols which results from a

series of phosphorylation and dephosphorylation is shown below (Figure 3.7). Most phosphatidic acids (PA) are autonomously synthesized by mitochondria⁵. Less is known with regard to PA however, PA may recruit cytosolic proteins, since it remains in the mitochondrial membrane. SM is enriched within plasma-membrane which indicates the concentration of SM probably plays an important role in forming the early endosome⁵.

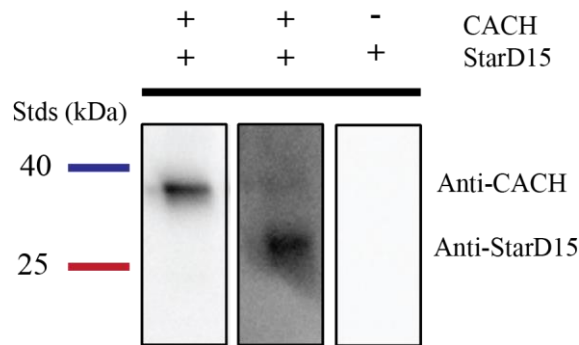


Figure 3.9 Western blots of the protein fraction eluted from CACH antibody-functionalized agarose beads incubated with 150 μ g of CACH and 100 μ g of StarD15. Lane 1 was treated with anti-CACH and lane 2 was treated with anti-StarD15. Lane 3 is the protein from the control in which CACH was omitted and treated with anti-StarD15. (middle+/+, Latham, unpublished data)

Considering the lipids interaction results found in StarD15, StarD15 may function as signal target which helps transport the two hotdog domain (CACH) to specific organelles. Most likely, CACH could be transported into endosome where catalyzes acyl-CoA to free coenzyme A. This process could be a crucial source of cellular coenzyme A.

Although Acot12 possesses more interaction with lipids, the binding efficiency is limited (Figure 3.7). Those extra binding lipids may result from structure difference when StarD15 and CACH link together. As described above, PI, PI(3)P, PI(4)P, PI(5)P, PI(3,4)P, PI(4,5)P and PI(3,4,5)P are plasma-membrane lipids. Thus, those more binding lipids could help enhance CACH transportation efficiency and localization accuracy. Moreover, the two trunked domains present high binding efficiency (Figure 3.8). In this case, communication between the two hotdog domain and StarD15 domain will be very interesting.

3.3.4 Site-directed mutagenesis

3.3.4.1 Mutants purification and verification

Of particular interest is the catalytic Asp which functions in either nucleophilic or base catalysis. The model indicates that CACH Asp31 assumes one or the other of these two roles. Based on this model the active site residues include Asp31 (presumed to act as the catalytic nucleophile or base), Glu205 (presumed to act to stabilize the CoA thiolate anion leaving group via hydrogen bond formation).

To analyze CACH catalytic mechanism, mutants were generated by replacing the active site residue. Since there are two active sites per CACH molecule, mutagenesis was designed as two stages. The first stage is aim to mutant the most important catalytic residues, Glu205 and Asp31, in two active sites individually. For the second stage,

double mutant was generated by using E205A or D31A plasmid as templates individually and mutant one of the catalytic residue in the other active site.

The CACH site-directed mutants were prepared by using a PCR-based strategy, and purified to homogeneity using a His6-tag Ni affinity column (SDS-PAGE gels are shown in Figure 3.10). The yields of the mutant proteins in mg protein per g of wet cells are as follows: D31A ~0.5 mg/g, E205A ~0.5 mg/g. The identity of each mutant protein was verified by ES-MS: D31A (calculated mass 36553.5Da; found 36553.1Da) and E205A (calculated 36539.5Da; found 36539.1Da).

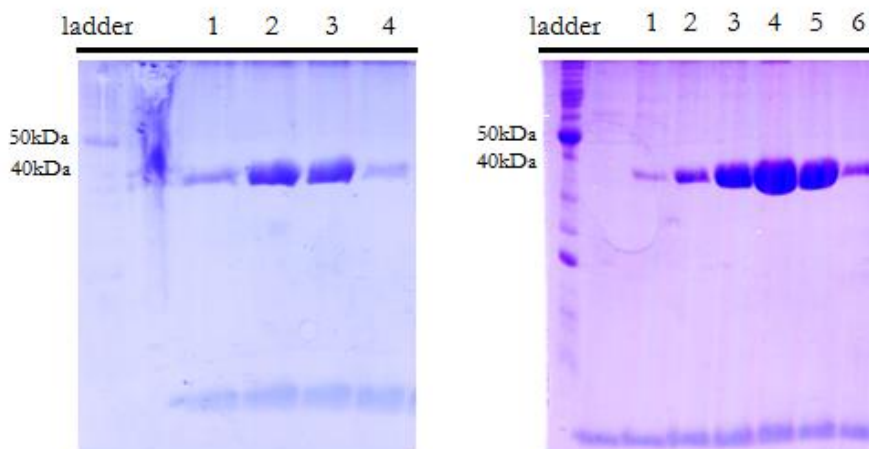


Figure 3.10 SDS-PAGE gel analyses of the CACH mutants containing fractions (A) D31A, (B) E205A pictured in the gel stained with Coomassie blue dye. See Materials and Methods for details

3.3.4.2 Kinetics study of CACH single mutants

Mutants E205A and D31A were synthesized and purified as described above. Table 3.3 shows the kinetics constants of CACH mutant catalyzed isobutyryl -CoA.

CACH Thioesterase			
Mutants	k_{cat} (s^{-1})	K_M (μM)	k_{cat}/K_M ($M^{-1}s^{-1}$)
WT	1.24 ± 0.06	56.3 ± 7.4	2.2×10^4
D31A	$(0.23 \pm 0.05) \times 10^{-1}$	23.1 ± 1.4	9.9×10^2
E205A	$(2.86 \pm 0.02) \times 10^{-1}$	25.4 ± 4.0	1.1×10^4

Table 3.2 Steady state kinetics study of CACH single mutants-catalyzed hydrolysis of isobutyryl-CoA substrate monitored by DTNB coupled reaction in 50mM HEPES at pH 7.5 and 25 °C.

K_m and k_{cat}/K_m value of CACH E205A were half way by comparing to wild-type CACH, although k_{cat} of CACH E205A was lower than the half k_{cat} of wild-type. This suggests that the two active sites share same catalytic significance.

However, the kinetics study of CACH D31A indicates that Asp31 is a more important catalytic residue than Glu205. For mutation on CACH Asp31, k_{cat} is much lower than the half k_{cat} of wild type, and K_{cat}/K_m decreased by twenty-fold, although K_m is around half way of wild-type K_m .

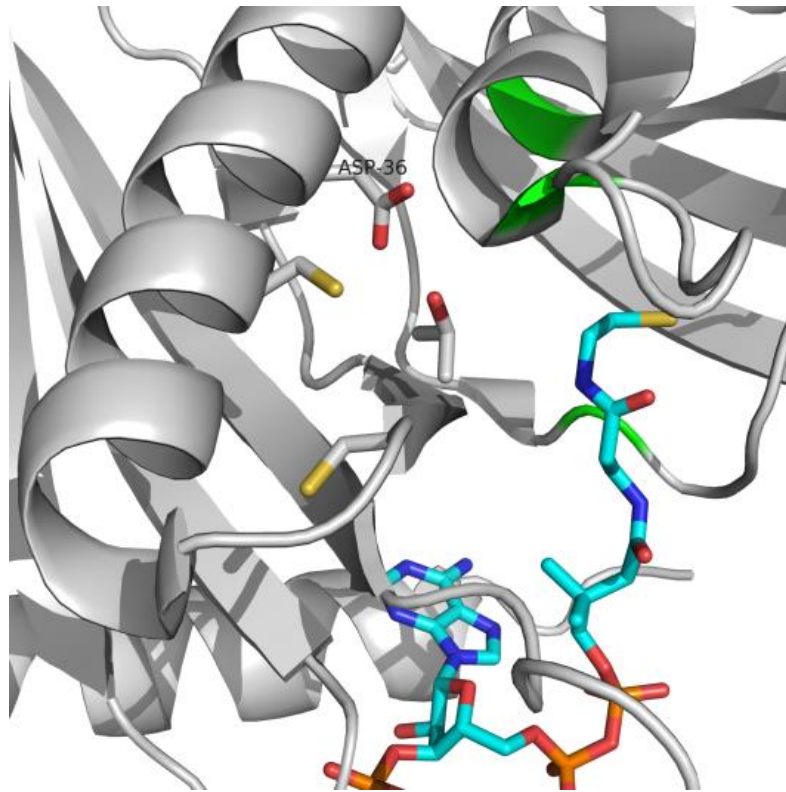


Figure 3.11 Cysteine residues nearby active site. Yellow color represents atom S which shows cysteine residues location.

There are two cysteine residues nearby the catalytic residues, Asp31 and Thr32, which may affect CACH catalytic efficiency (Figure 3.11).

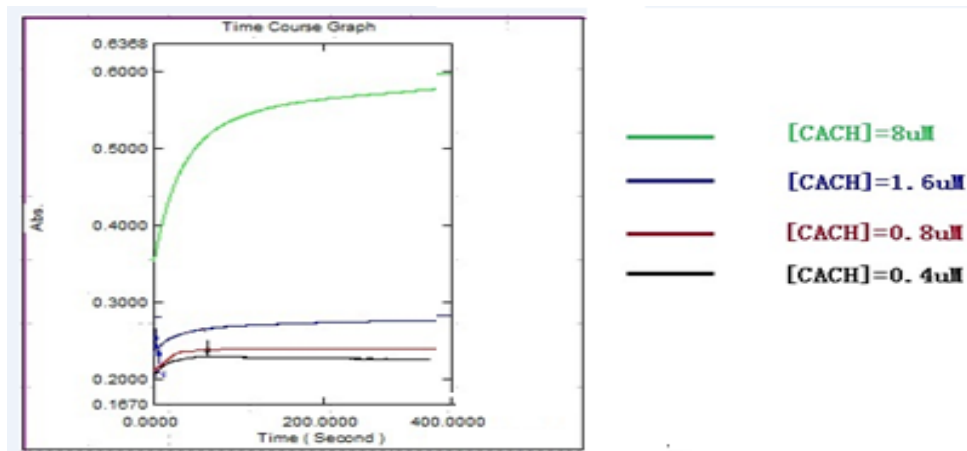


Figure 3.12 kinetics background study of wild-type CACH was measured using the DTNB spectrophotometric assay at pH 7.5 and 25 °C.

Due to the unexpected modification of CACH, the reliability of wild-type enzyme kinetics was tested by measuring out background (Figure 3.12). The reaction rates were correlated with CACH concentration. The higher concentration of wild-type CACH gave out higher reaction rates. This result indicates that the cysteine residues nearby the active site reacted with DTNB.

3.3.5 Discussion

Unlike YigI, CACH contains a steroidogenic acute regulatory (START) domain besides two hotdog domains. START domain is known as a lipid transporter. Thus, the function and regulation of CACH will be very interesting.

Chapter three focuses on the function two hotdog domain of CACH. CACH displays high activity on isobutyryl-CoA instead of acetyl-CoA, the predicted best substrate. However, this could be caused by the unexpected modification (cysteine residues nearby active site). The modification of CACH was observed under high enzyme concentration, while the substrate profile was determined under low enzyme concentration. Considering the high catalytic activity, CACH is still a functional enzyme. Thus, the method without DTNB need to be carried out to further provide the catalysis evidences. Also, since the cysteine residues are known effect on enzyme activity, mutagenesis on the cysteine residues would be necessary for the following study.

The results of lipid-protein binding assay give a hint of CACH function. However, CACH was expressed in *E coli*. which does not contain organelles. If CACH can be transported among organelles, expression in human cell lines will be necessary. More research that focuses on the location of the two hotdog-fold domain and the START domain might be interesting. Also, because full length CACH (Acot12) exhibits different protein-lipids interaction, START domain probably can regulate the structure when it binds to the two hotdog domain. Thus, research on Acot12 will be one of the goats for next step.

3.4 References

1. Kirkby, B.; Roman, N.; Kobe, B.; Kellie, S.; Forwood, J. K., Functional and structural properties of mammalian acyl-coenzyme A thioesterases. *Prog Lipid Res* **2010**, *49* (4), 366-77.
2. Westin, M. A.; Alexson, S. E.; Hunt, M. C., Molecular cloning and characterization of two mouse peroxisome proliferator-activated receptor alpha (PPARalpha)-regulated peroxisomal acyl-CoA thioesterases. *The Journal of biological chemistry* **2004**, *279* (21), 21841-8.
3. Westin, M. A.; Hunt, M. C.; Alexson, S. E., Short- and medium-chain carnitine acyltransferases and acyl-CoA thioesterases in mouse provide complementary systems for transport of beta-oxidation products out of peroxisomes. *Cellular and molecular life sciences : CMLS* **2008**, *65* (6), 982-90.
4. Krauss, M.; Haucke, V., Phosphoinositide-metabolizing enzymes at the interface between membrane traffic and cell signalling. *EMBO reports* **2007**, *8* (3), 241-6.
5. van Meer, G.; Voelker, D. R.; Feigenson, G. W., Membrane lipids: where they are and how they behave. *Nature reviews. Molecular cell biology* **2008**, *9* (2), 112-24.